Received: 29 October 2020 | Accepted: 14 November 2020

DOI: 10.1111/gcbb.12792

ORIGINAL RESEARCH

GCB-BIOENERGY BIOPRODUCTS FOR A SUSTAINABLE BIOECONOMY Open Access

WILEY

Assessing hydrologic and water quality effects of land use conversion to *Brassica carinata* as a winter biofuel crop in the southeastern coastal plain of Georgia, USA using the SWAT model

Nahal Hoghooghi[1] | **David D. Bosch**[2] | **Brian P. Bledsoe**[1]

[1]School of Environmental, Civil, Agricultural, and Mechanical Engineering, College of Engineering, University of Georgia, Athens, GA, USA

[2]Southeast Watershed Research Laboratory, U.S. Department of Agriculture, Agricultural Research Service, Tifton, GA, USA

Correspondence
Nahal Hoghooghi, School of Environmental, Civil, Agricultural, and Mechanical Engineering, College of Engineering, University of Georgia, Athens, GA 30602, USA.

Funding information
United States Department of Agriculture National Institute of Food and Agriculture, Grant/Award Number: SRD0007 and 2016-11231

Abstract

Carinata (*Brassica carinata*) is an industrial oilseed feedstock for renewable fuels grown as a winter crop in the southeast US, which may provide a new rotation alternative and benefits for water quality. However, the effects of carinata on water quantity and quality at the watershed and local scales are unknown. In this study, we use the Soil and Water Assessment Tool (SWAT) to assess the potential influence of carinata on water balance components, nutrients and sediment loads under plausible future scenarios of land use change in the upper Suwannee River Basin in the Atlantic Coastal Plain Physiographic Region near Tifton in South-Central Georgia. Three future scenarios are considered, including planting stand-alone carinata in winter fallow land every third year, planting stand-alone winter wheat in winter fallow land every third year, and carinata and winter wheat in rotation, one year of winter carinata followed by two years of winter wheat during simulation periods. The results show that under all three future scenarios, surface runoff, sediment, phosphorus, and nitrogen loadings decrease at both watershed and local scales, with higher average monthly reductions in the stand-alone carinata scenario versus the stand-alone winter wheat scenario. When carinata and winter wheat were planted over 36% of the total watershed area, reduction in total sediment, mineral phosphorus, and nitrate loads was ranging from 11.5% to 50.0%. However, when only 12% of the total watershed area was converted to carinata, the simulated reductions ranged from 3.8% to 14.0%. This suggests that the extent of carinata planting is crucial in assessing its hydrologic and water quality benefits. Overall, these results indicate that planting the biofuel carinata as a winter crop can reduce sediment and nutrient loading and provide water quality benefits to downstream waterbodies.

KEYWORDS

biofuel, carinata, nitrate load, sediment load, Soil and Water Assessment Tool (SWAT), total phosphorus load, water balance, watershed scale

1 | INTRODUCTION

Bioenergy crop production has been introduced globally as an alternative fuel source aiming to reduce greenhouse gas emissions and improve stream water quality. In the United States (US), the Energy Independence and Security Act of 2007 targets the production of 136 billion liters of renewable biofuel by 2022, with 58% to be derived from advanced biofuels (non-corn feedstocks) to obtain a 50% reduction in greenhouse gas emissions (USDA, 2010). There is a growing body of studies focused on the effect of the ethanol produced from corn grain and crop residue on hydrology and stream water quality (Demissie et al., 2017; Guo et al., 2018; Simpson et al., 2008). However, grain-based ethanol can promote competition among food, feed, and fuel. Moreover, removal of crop residue such as corn stover can increase soil erosion and stream water quality degradation (Hoekman et al., 2018; Shrestha et al., 2019). In addition, second-generation biofuels derived from non-food biomass that include lignocellulosic biomass can result in the depletion of soil carbon (Gerbrandt et al., 2016). However, advanced biofuels derived from specific feedstocks such as industrial oilseed crops may be used to eliminate the competition among food, feed, and fuel and have potential environmental benefits. Unlike second-generation biofuels, much of the biomass from advanced biofuels remains in the field after harvesting the seeds, which may increase soil carbon sink and reduce carbon emissions (Christ et al., 2020).

Carinata (*Brassica carinata*) is an off-season oilseed crop that has been introduced as a promising advanced feedstock for bio-based fuel industries. The oil is considered non-food oil because of the high erucic acid content (>40%) with long carbon chains which allows easier and more energy-efficient conversion to aviation fuel (Greene, 2017). Also, the crude protein produced as a result of carinata seed crushing can be used as a meal supplement for beef and dairy cattle (Schulmeister et al., 2019).

In the southeast US, carinata has been commercially grown as an off-season winter crop to produce aviation fuels on fallow lands, which increased revenue for farmers (Seepaul et al., 2019). Additionally, carinata may provide off-season crop benefits to the rotation, such as improved soil structure, reducing soil erosion, runoff, and nutrient leaching, and improved weed and disease control (Shah et al., 2017; Sharpley et al., 1991; Yasumoto et al., 2011). It was estimated th\at winter crops in *Brassica* family, such as *Brassica napus* L. (i.e., winter canola), can provide up to 80% canopy cover during the winter, an essential consideration for erosion control (Haramoto & Gallandt, 2004). However, carinata is more heat and drought tolerant than canola (Seepaul et al., 2016). *Brassica* crops are also capable of capturing excess nitrate after crop harvesting and reducing nitrate leaching into the soil profile (Baggs et al., 2000; Isse et al., 1999).

Research on carinata nutrient uptake responses to nitrogen (N) fertilizer with four N rates (0, 45, 90, and 135 kg N ha^{-1}) was conducted at the field trials (1.5 × 20 m) in the southeast US at Quincy, FL, on loamy fine sand soils. The authors found that total N uptake exceeded applied N by 11 to 160%, suggesting carinata is highly efficient at utilizing residual soil N (Seepaul et al., 2019). However, there is a scientific gap in the effects of carinata on surface runoff reduction, nutrient, and sediment loads at a larger scale, particularly in the Southeast United States.

Hydrologic models are ideal tools for predicting the hydrologic responses and nutrient and sediment loads for future scenarios at watershed scales. Soil and Water Assessment Tool (SWAT; Arnold et al., 2012) is one of the most broadly applied watershed models that has been used for evaluating the effects of biofuel-related scenarios on hydrology and water quality (Chen et al., 2017; Cibin et al., 2016; Engel et al., 2010; Holder et al., 2019). However, many bioenergy crops such as carinata are not represented in the SWAT plant database and other watershed models. To represent biofuel crops in the SWAT plant database, some used parameters from other crops available in the crop database of the model or used parameters derived from other crop model simulations (Miguez et al., 2012; Ng et al., 2010). To account for accurate estimation of plant parameters such as plant nutrient uptake and leaf area development, which affect the outputs of hydrologic and water quality models, it is crucial to use evidence-based values from field studies in a similar region (Trybula et al., 2015).

Our objective was to assess the potential impacts of plausible carinata scenarios as a winter crop on watershed hydrology and water quality using the SWAT model in Coastal Plain of Georgia, US. The specific objectives were to: (1) set up a carinata plant database in the model and develop plausible carinata scenarios as a winter crop standalone and in combination with the most common small grain winter crop in the southeast US (winter wheat) using the SWAT model, (2) assess potential benefits of the land use change from fallow to carinata on evapotranspiration (ET), surface runoff, percolation, water yield, total nitrogen (TN), nitrate (NO_3-N), total phosphorus (TP), soluble P, mineral and organic P attached to the sediment, and sediment loads, and (3) compare and contrast the hydrologic responses and water quality benefits of carinata at both watershed scale and Hydrologic Response Unit (HRU) level (hereafter we call it local scale). Our study is one of the first, to our knowledge, to fill these scientific gaps using the process-based semidistributed hydrologic SWAT model in the southeast US.

2 | MATERIALS AND METHODS

2.1 | Study area

We conducted this study at the ~334 km^2 Little River Experimental Watershed (LREW) in the Coastal Plain of

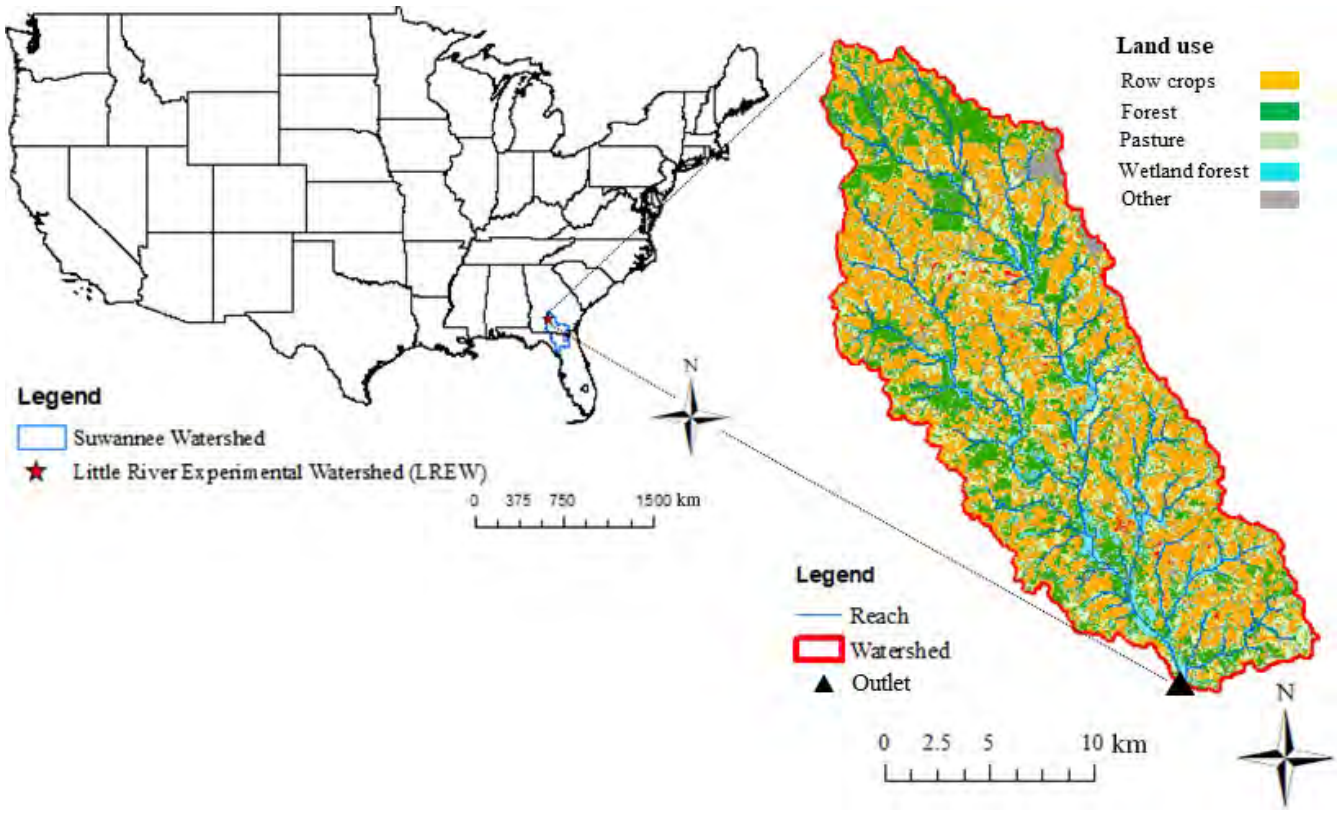

FIGURE 1 Little River Experimental Watershed is located at the headwater of the upper Suwannee River watershed in the Coastal Plain Physiographic Province near Tifton in South-Central Georgia, US. The triangle represents the outlet of the watershed

Georgia, in the southeast US (Figure 1). The LREW is located in the headwaters of the Suwannee River Basin and flows in a south direction, eventually joining the Suwannee River which drains into the Gulf of Mexico. The LREW was instrumented by the United States Department of Agriculture, Agriculture Research Service (USDA-ARS) to measure streamflow and water quality (Bosch et al., 1999).

The LREW climate is categorized as humid subtropical with a long growing season. High-intensity rainfall with short-duration promotes runoff and erosion that may carry soluble and adsorb nutrient particles of applied fertilizers and pesticides into surface waters (Bosch et al., 2004). The surface soil texture in the LREW is mainly sands and sandy loams with a high infiltration rate, underlain by limestones that form the Floridan Aquifers (Bosch et al., 2007). The Floridan aquifer in this area is generally confined, and stream networks are not incised into deeper groundwater. The LREW is dominated by a dense dendritic network of stream channels with channel slopes of less than 5% bordered by riparian forest wetlands (Cho et al., 2010). The average annual precipitation and temperature are 1208 mm and 19.1°C, respectively.

The LREW consists of mixed land use. Dominant land uses are 42% row crops (36% peanut and cotton, and 6% winter wheat), 34% forest (evergreen and deciduous), 10% pasture, 9% wetland forest, and 5% other (urban and water). There are no permitted point source discharges in the LREW (Feyereisen et al., 2007).

2.2 | Model description

We used the process-based, sem-idistributed, and continuous time-step SWAT to simulate hydrology, crop growth, nutrient, and sediment loads (Arnold et al., 2012). In SWAT, a watershed is divided into subbasins which are further divided into HRUs consisting of homogeneous land use, soil type, and slope. The hydrologic processes of a watershed in SWAT are divided into two major phases: the first phase is the land phase, which controls the amount of water, sediment, nutrient, and pesticide loading to the main channel in each subbasin. The second phase is the water routing phase, which simulates the movement of water, sediment, etc., through the channel network of the watershed to the outlet. The hydrologic cycle in SWAT is based on the water balance equation:

$$\mathrm{SW}_t = \mathrm{SW}_0 + \sum_{i-1}^{t} (R_{\mathrm{day}} - Q_{\mathrm{surf}} - E_{\mathrm{a}} - w_{\mathrm{seep}} - Q_{\mathrm{gw}}),$$

where SW_t is the final soil water content (mm), SW_0 is the initial soil water content on day i (mm), t is the time (days), R_{day} is the amount of precipitation on day i (mm), Q_{surf} is

the amount of surface water on day i (mm), E_a is the amount of precipitation on day i (mm), w_{seep} is the amount of infiltration from the bottom of the soil profile to the vadose zone on day i (mm), and Q_{gw} is the amount of groundwater contribution to the stream on day i (mm; Arnold et al., 2012).

We used the Soil Conservation Service (SCS) curve number (CN) method to predict surface runoff (SCS, 1972). Following Liew et al. (2005), we chose the Hargreaves method (Hargreaves et al., 1985) to estimate potential evapotranspiration at the LREW.

We used ArcSWAT 2012 interface for ArcGIS 10.3.2 platform. To set up the SWAT model for the LREW we used 30-m Digital Elevation Model, Soil Survey Spatial Tabular (SSURGO 2.2) soils data, National Land Cover Dataset, and National Agricultural Statistics Services for land use data. Daily precipitation, temperature, relative humidity, solar radiation, and wind data were obtained from Global Weather Data for SWAT (NCEP, 2014). We used the threshold values of 20%, 10%, and 5% of the subbasin area for soil, land uses, and slope classes, respectively. Then LREW was delineated to 198 subbasins and 1272 HRUs.

2.3 | Management practices of crops

We set up a baseline SWAT model with the most common summer crop practices of a 3-year cotton, cotton, and peanut rotation in the southeast US, specifically in Georgia and Florida. The crop management parameters such as tillage, planting, fertilizer application, harvesting were scheduled by date using the University of Georgia Cooperative Extension services for Tift County (UGA Extension, 2005; Table 1). The amount of 65 kg N ha^{-1} in the form of elemental nitrogen fertilizer and 50 kg P ha^{-1} of phosphorus fertilizer as P_2O_5 (phosphorus pentoxide) was applied in cotton fields. No cover crops were planted during winter for the baseline simulation.

A base flow separation technique (Arnold et al., 1995) was used to initiate the value of the base flow recession constant (ALPHA_BF). We made relative adjustments of ALPHA_BF during the model calibration.

TABLE 1 Simulated management practices for cotton, peanut, carinata, and winter wheat in SWAT

Operations	Date	Input data
Cotton		
Tillage	May 30	Deep ripper subsoiler
Fertilizer	N fertilizer: June 28 P fertilizer: June 30	Anhydrous ammonia: 67 kg N ha^{-1} Elemental phosphorus: 50 kg P ha^{-1}
Planting	May 31	
Harvest and kill	November 30	
Peanut		
Tillage	May 30	Deep ripper subsoiler
Planting	May 31	
Harvest and kill	November 15	
Carinata		
Tillage	December 01	Single disk
Fertilizer	N fertilizer: December 02, February 25, and March 20 P fertilizer: December 02	Ammonium nitrate: 22.5, 45, and 22.5 kg N ha^{-1} Elemental phosphorus: 56 kg N ha^{-1}
Planting	December 02	
Harvest and kill	May 29	
Winter wheat		
Tillage	December 01	Single disk
Fertilizer	December 02 and February 20	Ammonium nitrate: 25 and 65 kg N ha^{-1}
Planting	December 02	
Harvest and kill	May 28	

Note: Date of each operation and input data were based on the University of Georgia Cooperative Extension services for Tiff County, Georgia (UGA Extension, 2005).

Abbreviation: SWAT, Soil and Water Assessment Tool.

2.4 | Baseline model calibration, validation, and uncertainty analysis

The Sequential Uncertainty Fitting algorithm (SUFI-version 2) in the SWAT Calibration and Uncertainty Program platform was used (Abbaspour, 2013) to calibrate and validate the base model for streamflow, sediment, TP, and NO_3-N loads. We used measured USDA-ARS daily streamflow and nutrient loads at the main LREW outlet from 1997 to 2005 for model calibration and validation from the SEWRL database (Bosch et al., 2007). Calibration and validation were only conducted at the watershed scale. The SUFI-2 combines optimization with uncertainty analysis. Uncertainties in the parameters result in the model output uncertainties which are quantified as the 95% prediction uncertainty (95 PPU) band between the 2.5% and 97.5% levels of the cumulative distribution of an output variable using Latin Hypercube sampling (Abbaspour et al., 2007). We used a 4-year initialization (1993–1996) followed by a 5-year calibration (1997–2001), and a 4-year validation (2002–2005) for the base model.

We selected two quantitative error statistics Kling-Gupta Efficiency (KGE; Gupta et al., 2009) and Percent Bias (PBIAS), to evaluate the model performance.

The KGE contains three components: correlation (r), present bias (μ_s/μ_o), and variability ratio (σ_s/σ_o) between the simulated (s) and observed (o) variable, μ and σ are the mean and SD of the variable, respectively:

$$\mathrm{KGE} = 1 - \sqrt{\left\{ (r-1)^2 + \left(\frac{\mu_s}{\mu_o} - 1\right)^2 + \left(\frac{\sigma_s}{\sigma_o} - 1\right)^2 \right\}},$$

and KGE ranges from $-\infty$ to 1, with a value closer to 1 represents a relatively accurate model. KGE overcomes the disadvantage of Nash-Sutcliffe efficiency (Nash & Sutcliffe, 1970) in underestimating peak flows prediction (Gupta et al., 2009). PBIAS measures the average tendency of the predicted data to be larger or smaller than observed values. It also measures overestimation and underestimation of bias (Moriasi et al., 2007):

$$\mathrm{PBIAS} = \frac{\sum_{i=1}^{n} (O_i - S_i)}{\sum_{i=1}^{n} O_i} \times 100.$$

The optimum value for PBIAS is 0%, where values close to zero indicate better model prediction and overestimation is signified by PBIAS <0% and underestimation indicates when PBIAS >0% (Moriasi et al., 2015).

Previous research in LREW has examined the application of the SWAT model to the LRWE with different approaches (Bosch et al., 2004; Feyereisen et al., 2007; Liew et al., 2005). Yet, we identified hydrology parameters used in our model calibration procedure from the aforementioned SWAT literature in this experimental watershed. In addition to these parameters, we incorporated relevant biophysical parameters (Rajib et al., 2018) for major crops in the LREW in our calibration process. Also, parameters controlling nutrients and sediment loads were indicated through a literature review (Abbaspour et al., 2007; Cho et al., 2010; Moriasi et al., 2012). Parameters controlling streamflow and plant growth were calibrated first, followed by sediment and phosphorus, and then nitrogen parameters.

Because ET is considered an important component of the hydrologic and plant growth cycle, we used remotely sensed ET data to evaluate the spatial variability of the model (Herman et al., 2018). We used a year-end gap-filled yearly composite ~500 m gridded remotely sensed total ET data from Moderate Resolution Imaging Spectroradiometer MOD16A3GF version 6 from 2000 to 2005 (Running et al., 2019). The data were corrected according to the scale factor and spatially aggregated into each of the 198 subbasins of the LREW. Then, relative error with respect to simulated total ET was calculated for each subbasin at the LREW.

2.5 | Scenarios representation in the SWAT model

The calibrated baseline model was used to represent carinata scenarios. Carinata was selected as a winter crop for this study region to replace winter fallow land in cotton and peanut land uses. Carinata needs to be rotated with other crops and not be planted in the same field for at least two consecutive years to avoid or minimize disease and nematodes (Seepaul et al., 2016). Also, planting carinata after peanut is not recommended due to the leftover pesticide from peanut production that may develop diseases in carinata. Therefore, in our model, carinata was planted after cotton rotation during the winter growing season.

A recommended planting date for carinata in the southeast is between November 1 and November 30 (Seepaul et al., 2016). In our model, carinata was planted on December 02 and harvested on May 29 every 3 years. At the harvest, much of the biomass remains in the field after seeds are harvested. The harvest index (HVSTI) was calculated as the ratio of seed to the total aboveground biomass at seed maturation and set to 0.35 in the SWAT plant database (Seepaul et al., 2019).

A recommended fertilizer application rate of about 90 kg N ha^{-1} in the form of ammonium nitrate (NH_4NO_3, 34-0-0) was applied in three applications with 25% at planting, 50% at bolting, and 25% at flowering (Seepaul et al., 2019). A 56 kg P ha^{-1} fertilizer in the form of triple superphosphate ($Ca(H_2PO_4)$, 0-44-0) was applied at the time of planting (Table 1; Agrisoma, 2017–18).

To compare the potential benefits of carinata with other small grain winter crops, we added winter wheat to the crop rotation. Winter wheat is one of the most common winter crops planted in the southeast US for grain production and has almost minimum N fertilizer requirements as carinata (UGA Extension, 2005). Planting time for most winter wheat varieties grown in Upper Coastal Plain was ranging from November 07 to December 01 (UGA Extension, 2005). In our model, winter wheat was planted on December 02 (to allow 6 months growth period for cotton) and harvested on May 28. The minimum recommended fertilizer application rate for Tifton, Georgia, is 90 kg N ha^{-1} in the form of ammonium nitrate (NH_4NO_3, 33-0-0) with a 25% application at planting time and 75% prior to stem elongation (Table 1; UGA Extension, 1999). Winter wheat scenarios were implemented stand-alone and in combination with carinata.

The three simulated scenarios were:

S-C: Stand-alone winter carinata planted every third year, replacing winter fallow on Dec 1997–May 1998, Dec 2000–May 2001, and Dec 2003–May 2004.
S-W: Stand-alone winter wheat planted every third year, replacing winter fallow on Dec 1997–May 1998, Dec 2000–May 2001, and Dec 2003–May 2004.
S-CW: Carinata and winter wheat in rotation, one year of winter carinata followed by two years of winter wheat; Carinata replaced for winter fallow land on Dec 1997–May 1998, Dec 2000–May 2001, and Dec 2003–May 2004, and winter wheat replaced for winter fallow land on Dec 1998–May 1999, Dec 1999–May 2000, Dec 2001–May 2002, Dec 2002–May 2003, and Dec 2004–May 2005.

There were no changes in summer crop rotations relative to the baseline model in all three scenarios. For scenarios S-C and S-W, winter fallow conditions existed one-third of the time, while for scenario S-CW, no winter fallow conditions existed in fields with row crops.

Accurate representation of carinata phenology in SWAT requires specific crop growth parameters and management practices. Therefore, we obtained values for maximum potential leaf area index (BLAI), HVSTI, maximum canopy height (CHTMX), maximum root depth (RDMX), optimal temperature, and minimum (base) temperature for plant growth (T_OPT and T_BASE), normal fraction of nitrogen and phosphorus in yield (CNYLD and CPYLD), and normal fraction of nitrogen and phosphorus in plant biomass at emergence, 50% maturity, and maturity from Seepaul et al. (2019) from field measurements for carinata on loamy sand at University of Florida, North Florida Research and Education Center at Quincy, Florida and personal communications (Seepaul, 2018–19; Table 2). Other plant growth parameters such as radiation use efficiency (BIO_E) and maximum stomatal conductance (FRGMAX) were set to values for canola (*B. napus*), the same family as carinata, from the SWAT database (Arnold et al., 2013; Seepaul et al., 2016).

TABLE 2 Model inputs in the SWAT plant database relating to carinata growth and aboveground biomass nutrient content parameters (N, nitrogen; P, phosphorus). Values were obtained from field measurements at Quincy, Florida, in 2014 and 2015 (Seepaul et al., 2019)

Input description	Code in SWAT	Value
Maximum potential leaf area index	BLAI	6.37
Harvest index	HVSTI	0.35
Maximum canopy height (m)	CHTMX	1.2
Maximum root depth (m)	RDMX	0.3
Optimal temperature for plant growth (°C)	T_OPT	28
Base temperature for plant growth (°C)	T_BASE	0
Fraction of N in yield	CNLYD	0.04
Fraction of P in yield	CPYLD	0.009
Fraction of N in biomass at emergence (kg N kg^{-1} biomass)	BN1	0.0225
Fraction of N in biomass at 50% maturity (kg N kg^{-1} biomass)	BN2	0.0181
Fraction of N in biomass at maturity (kg N kg^{-1} biomass)	BN3	0.0101
Fraction of P in biomass at emergence (kg P kg^{-1} biomass)	BP1	0.0032
Fraction of P in biomass at 50% maturity (kg P kg^{-1} biomass)	BP2	0.0017
Fraction of P in biomass at maturity (kg P kg^{-1} biomass)	BP3	0.0015

The potential benefits of these land management changes on hydrology and nutrient loads over the period of 1997 to 2005 were assessed relative to the baseline condition both at the watershed and local (HRU level) scales. The monthly averages were calculated by averaging daily values within a month.

3 | RESULTS

3.1 | Baseline model calibration, validation, and uncertainty analysis

The calibration process for the LREW started with 36 hydrologic and biophysical parameters. After 1000 simulations, the most sensitive flow parameters were identified and listed in Table S-C in order of decreasing sensitivity. The most sensitive parameters were: effective hydraulic conductivity of the alluvium in the main channel (CH_K2.rte), runoff CN 2 (CN2.mgt), groundwater delay time (GW_DELAY.gw),

plant uptake compensation factor (EPCO), and available water capacity of the soil layer (SOL_AWC.sol; Table S1). CN2 for the main crops and forest (evergreen and deciduous) were reduced by 5% resulting in a better adjustment to streamflow predictions. Among biophysical parameters, radiation use efficiency (BIO_E) for wetland forest land use, and BLAI for pasture land use were the most sensitive parameters (Table S1). The daily KGE for streamflow is 0.75 with PBIAS of 5.1 for the calibration period and the KGE of 0.71 with a PBIAS of −1.0 for the validation period (Table 3; Figure 2). The observed streamflow, the model best fit, and the 95 PPU band for calibration and validation periods are shown in Figure 2.

The relative error in predicted ET in respect to remotely sensed ET data at the subbasin level is shown in Figure S1 in the supplemental material. The relative error for all 198 subbasins ranged from −27% to 28% with the RMSE (Root Mean Square Error) of 79 mm year^{-1} (11%; Figure S1).

After the model was calibrated for hydrology and biophysical parameters, the narrow ranges for these parameter values were fixed, and the model was calibrated for total suspended solids load at the watershed outlet using 14 parameters. Following calibration of the total suspended solids load, TP and nitrate (NO_3-N) loads were calibrated.

The most sensitive parameters for total suspended solids load were exponent parameter for calculating sediment reentrained in channel sediment routing (SPEXP.bsn), linear parameter for calculating the maximum amount of sediment that can be reentrained during channel sediment routing (SPCON.bsn), and the cover factor for the effect of land cover on erosion (USLE_C.plant; Table S1). The SPEXP and SPCON are parameters used to calculate the maximum amount of sediment that can be transported from a reach. The fitted value for SPEXP and SPCON in our model was 1.54 and 0.001, respectively. The daily KGE was 0.45 and 0.38 for the calibration and validation period, respectively with PBIAS of −6.0% for the calibration period and −12.3% for the validation period (Table 3; Figure3a). A lower KGE for the validation period was expected because the observation data for total suspended solids loads were sparse for that period (compared with daily observations for streamflow).

The most sensitive P parameters were phosphorus enrichment ratio for loading with sediment (ERORGP.hru), and soil erodibility factor (USLE_K.sol) (Table S1). The fitted values for ERORGP and USLE_K were 0.68 and 0.19, respectively. The daily KGE for TP load is 0.57 with PBIAS of −1.7% for the calibration period and the KGE of 0.37 with PBIAS of −5.2% for the validation period (Table 3; Figure 3b). The same as total suspended load, a lower KGE for the validation period was expected because the observation data for TP loads were sparse for the validation period.

Following the calibration of total suspended solids and TP loads, the model was calibrated for NO_3-N load. The most sensitive N parameter was denitrification threshold water content (SDNCO.bsn) (Table S1). The fraction of NO_3 in the soil surface layer that is lost to runoff relative to the amount removed via percolation parameter was not sensitive (NPERCO.bsn). The fitted value indicated that concentrations in surface runoff were 11% of the concentrations in the surface layer. Therefore, this parameter reduced NO_3 runoff losses. The daily KGE for NO_3-N load is 0.35, with PBIAS of −18.3% for the calibration period and the KGE of 0.44 with PBIAS of −0.3% for the validation period (Table 3; Figure 3c).

3.2 | Watershed level effects of carinata on hydrology and water quality

3.2.1 | Effects of carinata as a winter crop on hydrology

Simulated seed yield for carinata from cotton and peanut HRUs averaged 1752 kg ha^{-1} under S-C and S-CW scenarios. Simulated yield for carinata was similar to measured seed yield of 1794 kg ha^{-1} for Avanaz 641 variety from

TABLE 3 Observed and simulated streamflow, sediment, TP, and NO_3-N loads and daily statistical parameters for the baseline model during calibration and validation periods at the outlet of LREW

	Streamflow (m^3 year^{-1})	Sediment (tonne year^{-1})	TP (kg year^{-1})	NO_3-N (kg year^{-1})
Observed	925	483	11,241	21,169
Simulated	920	484	10,620	23,121
Calibration				
KGE	0.75	0.47	0.57	0.35
PBIAS	5.1	−6.0	−1.7	−18.3
Validation				
KGE	0.71	0.38	0.37	0.44
PBIAS	−1.0	−12.3	−5.2	−0.3

Abbreviations: KGE, Kling-Gupta Efficiency index; NO_3-N, nitrate- nitrogen; PBIAS, percent bias; TP, total phosphorus.

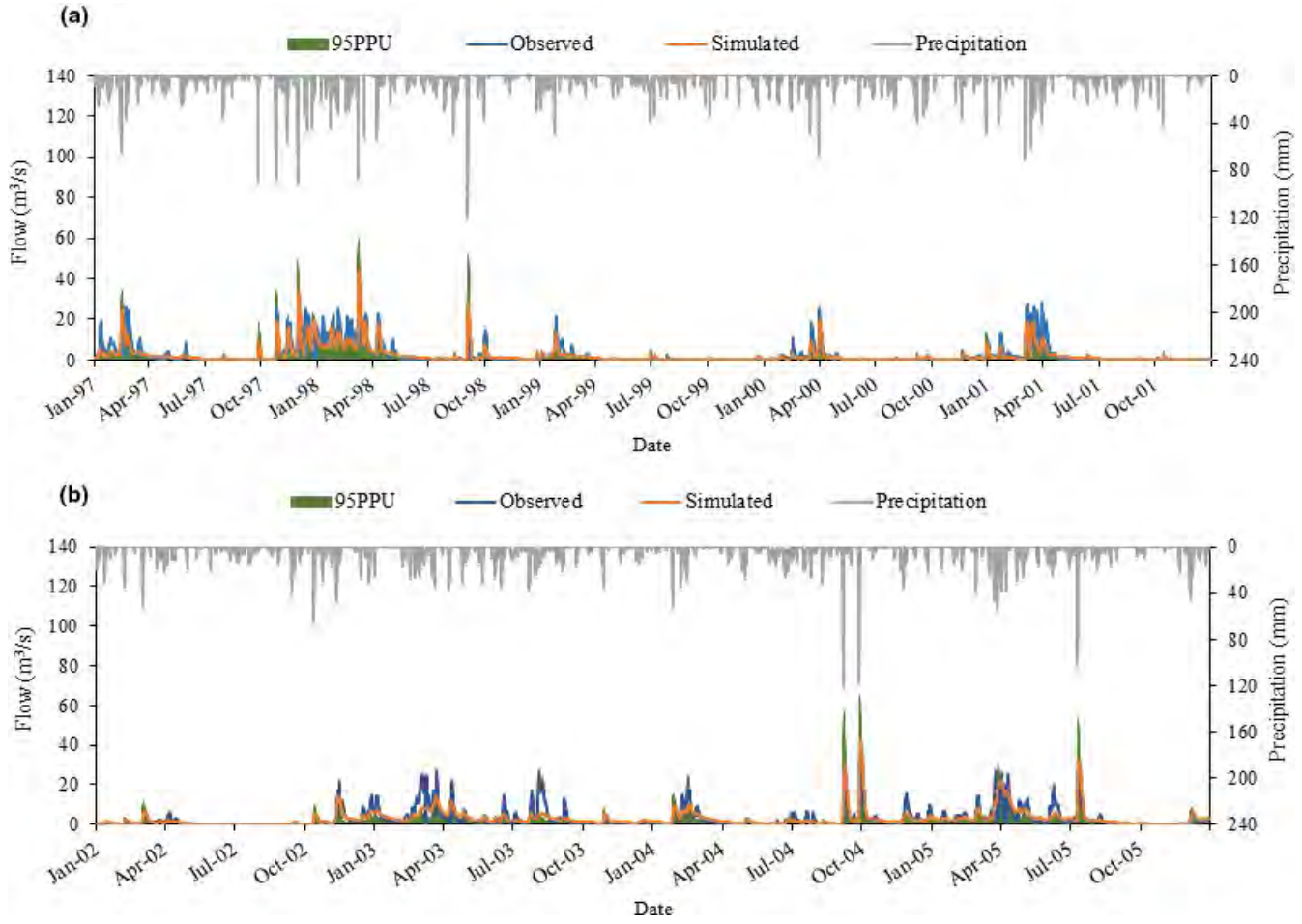

FIGURE 2 The daily observed streamflow, the model best fit, and 95 PPU band for Calibration (1997–2001) (a) and validation (2002–2005) (b) periods at the outlet of Little River Experimental Watershed. 95PPU, 95% prediction uncertainty

2019 to 2020 in Tifton, Georgia. Seepaul et al. (2020) reported carinata seed yields of 2300 kg ha^{-1} with N fertilizer application rate of 90 kg N ha^{-1} in a 5-year field study in Quincy, Florida. The simulated average winter wheat grain yield was 3600 kg ha^{-1} under S-W and S-CW scenarios. The late-planted winter wheat grain yield for Tifton, Georgia, from 1999 to 2000 was ranging from 3800 to 4900 kg ha^{-1} depends on wheat variety (UGA Extension, 1999).

Results at the watershed scale showed on average (1997–2005) about 64% of the precipitation was lost to ET (Table 4a) at the baseline condition. Under all scenarios (S-C, S-W, and S-CW), the increase in average annual ET compared to the baseline was negligible, ranging from 0.1 to about 1% (Table 4a). The small increase in average annual ET caused reductions in the annual surface water, water yield, and percolation by about 0.8%–1.4%, 0.2%–1.8%, and 0.2%–1.9%, respectively, compared to the baseline model for all scenarios; with the highest reduction simulated for S-CW (Table 4a).

Figure 4 shows the average monthly percent changes from 1997 to 2005 (December–May) on hydrology, N, P, and sediment loads relative to the baseline under different winter cover crop scenarios at the watershed outlet. From December to May, the average ET increased by 6.0 ± 1.2%, 2.4 ± 0.9%, and 1.0 ± 0.3% for S-CW, S-C, and S-W scenarios compared to baseline, respectively. Therefore percent changes in surface runoff from December to May at the downstream watershed outlet, ranging from 0.0%–25.0% with the mean reduction of 4.0 ± 0.9% under S-CW scenario, 0.0% to −25.0% with the mean reduction of 1.8 ± 0.7% under S-C scenario, and 1.7 to −3.7% with the mean of −0.5 ± 0.1% under S-W scenario (Figure 4a).

When compared to the baseline, simulated water percolation past the bottom of the soil profile decreased, with the highest reduction under S-CW scenario with the average reduction of 6.1 ± 2.0%, followed by S-C scenario (4.2 ± 2.0%), and S-W scenario (0.6 ± 0.6%) (Figure 4a). As a result, the simulated average water yield from December to May also reduced about 3.5 ± 0.5% (S-CW), 1.1 ± 0.3% (S-C), and 0.5 ± 0.1% (S-W) (Figure 4a).

There were no significant changes in average monthly water balance components from the following summer growing seasons under all three scenarios compared to the baseline at the outlet of LREW.

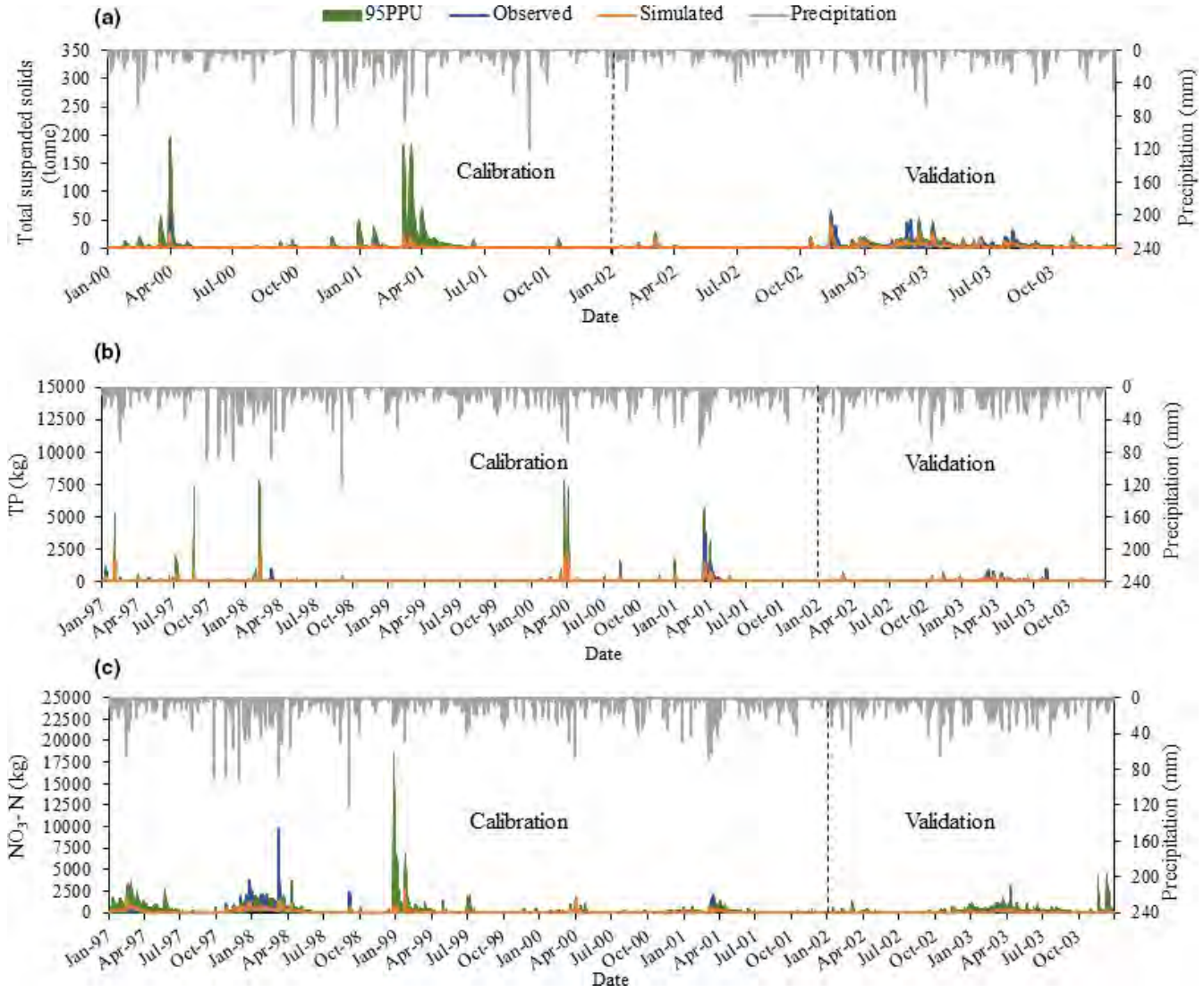

FIGURE 3 The daily observed, the model best fit, and 95 PPU band for total suspended solids (a), TP (b), and NO_3-N (c) loads at the outlet of Little River Experimental Watershed. 95PPU, 95% prediction uncertainty

3.2.2 | Effects of carinata on sediment, TP, and TN loads

At the watershed outlet, the average annual (1997–2005) total sediment load under S-C, S-W, and S-CW scenarios decreased by 4.2%, 1.5%, and 12.9%, respectively, compared to the baseline as a result of the reduction in average annual surface runoff (Table 4a). As a result, the average annual soluble mineral P transported by surface runoff decreased by 14% under S-C and S-W scenarios and 43% under the S-CW scenario (Table 4a).

The average annual (1997–2005) NO_3-N load through the surface runoff was reduced by 50% under scenario S-CW compared to the baseline (Table 4a). The decrease in surface runoff and increases in ET were the key drivers of reduced NO_3-N load in surface runoff. However, under S-C and S-W scenarios, the reduction in average annual (1997–2005) NO_3-N load in surface runoff compared to the baseline was small (Table 4a). Besides, the average annual NO_3-N leaching from the bottom of the soil profile was much higher than the average annual NO_3-N lost through surface runoff (45.3 kg ha^{-1} vs. 2.6 kg ha^{-1} for the baseline) at the downstream watershed outlet (Table 4a). Although the annual average percolation reduced only about 2% under S-CW scenario relative to the baseline (Table 4a), the NO_3-N leaching reduced by almost 40% under S-CW scenario due to higher plant N uptake (222 kg N ha^{-1} for S-CW vs. 179 kg N ha^{-1} for baseline). However, under stand-alone carinata scenario (S-C) and stand-alone winter wheat scenario (S-W), the reduction in average annual NO_3-N leaching relative to baseline was small and about −1% (Table 4a).

With the presence of carinata (S-C) and winter wheat (S-W), the average monthly (December–May) sediment load reduced about 6.0 ± 2.4% and 3.5 ± 2.2% compared to the

TABLE 4 Comparison of the average (1995–2007) annual water balance, nitrogen (N), phosphorus (P), and sediment parameters under baseline, stand-alone carinata (S-C), stand-alone winter wheat (S-W), and rotating carinata and winter wheat (S-CW) scenarios at the watershed outlet (a), and cotton and peanut HRUs (b). The number in parentheses is the percent change relative to the baseline condition (winter fallow)

	Baseline	S-C	S-W	S-CW
(a) Entire watershed				
Precipitation (mm)	1125.8	1125.8	1125.8	1125.8
ET (mm)	718.1	722.2 (0.6)	719.1 (0.1)	725.2 (0.9)
Surface runoff (mm)	94.9	94.1 (−0.8)	94.6 (−0.3)	93.6 (−1.4)
Percolation (mm)	278.0	274.9 (−1.1)	277.3 (−0.2)	272.5 (−1.9)
Water yield (mm)	408.4	404.3 (−1.0)	407.4 (−0.2)	401.1 (−1.8)
Total sediment (tonne ha^{-1})	2.60	2.50 (−3.8)	2.56 (−1.52)	2.3 (−11.5)
Soluble P (kg P ha^{-1})	0.14	0.12 (−14.3)	0.12 (−14.3)	0.08 (−42.8)
NO_3-N load in surface runoff (kg ha^{-1})	2.6	2.5 (−3.8)	2.5 (−3.8)	1.3 (−50.0)
NO_3-N leaching (kg ha^{-1})	45.3	45.0 (−0.6)	44.9 (−0.8)	27.0 (−40.3)
(b) Cotton and peanut HRUs				
Precipitation (mm)	1125.8	1125.8	1125.8	1125.8
ET (mm)	671.9	682.9 (1.6)	674.6 (0.4)	690.8 (2.8)
Surface runoff (mm)	129.6	127.6 (−1.5)	128.9 (−0.5)	126.3 (−2.5)
Percolation (mm)	262.9	254.6 (−3.2)	261.0 (−0.7)	248.6 (−5.4)
Water yield (mm)	444	433.0 (−.2.5)	441.4 (−0.6)	424.9 (−4.3)
Total sediment (tonne ha^{-1})	4.7	4.4 (−6.4)	4.6 (−2.1)	3.6 (−23.4)
Mineral P attached to sediment (kg P ha^{-1})	0.8	0.6 (−25.0)	0.6 (−25.0)	0.4 (−50.0)
Soluble P (kg P ha^{-1})	0.3	0.2 (−33.3)	0.2 (−33.3)	0.1 (−66.7)
NO_3-N load in surface runoff (kg N ha^{-1})	5.5	5.4 (−1.8)	5.4 (−1.8)	2.2 (−60.0)
NO_3-N leaching (kg N ha^{-1})	96.1	95.1 (−1.0)	95.1 (−1.0)	53.4 (−44.4)

baseline at the watershed outlet (Figure 4b). Under S-CW scenario, the average monthly sediment load reduction was the highest, with 12.0 ± 3.3% reduction relative to the baseline (Figure 4b). Under all three scenarios, as a result of plant residue remaining from the previous winter growing season, detachment of soil particles and therefore sediment loading to the stream also decreased for the following summer crops about 7.0 ± 2.1%, 4.0 ± 2.7%, and 3.6 ± 2.1% for S-CW, S-C, and S-W scenarios, respectively (data not shown).

At the downstream outlet, the average monthly NO_3-N and soluble P loads in surface runoff from December to May (1997–2005) decreased mainly due to the reduction in average surface runoff (Figure 4a,b). The highest reduction in NO_3-N and soluble P loads observed under S-CW scenarios, with 34.6 ± 5.2% and 24.4 ± 5.6%, respectively (Figure 4b). A higher reduction in simulated soluble P in surface runoff was observed under S-C scenario (10.0 ± 4.0%) compared to S-W scenario (1.2 ± 1.2%; Figure 4b). Reduction in surface runoff NO_3-N for S-W and S-C scenarios was almost the same and about 13.4 ± 4.0% and 12.0 ± 3.8%, respectively.

Soluble P loading from the following summer growing seasons decreased by 10.3 ± 4.0% under S-CW and 1.0 ± 0.9% under S-C due to higher availability of mineral P for plant uptake relative to winter fallow (baseline). Under S-W scenario, we did not observe any changes in soluble P load from following summer growing seasons.

As percolation into shallow aquifer decreased (Figure 4a), the average monthly (December–May) NO_3-N load through leaching also reduced relative to the baseline. Again, the highest reduction occurred under S-CW scenario relative to the baseline, where NO_3-N load from leaching decreased by 23.2 ± 4.4% (Figure 4b). The average monthly NO_3-N leaching from the following summer growing seasons reduced about 6.5 ± 4.0% under S-CW, and 2.6 ± 3.0% under S-C and S-W scenarios.

3.3 | Local level effects on hydrology and water quality

3.3.1 | Effects of carinata winter crop on hydrology

Hydrologic Response Unit (HRU) level analyses were assessed to indicate the local level benefits of the carinata production on hydrology and water quality. Figures 3 and 4

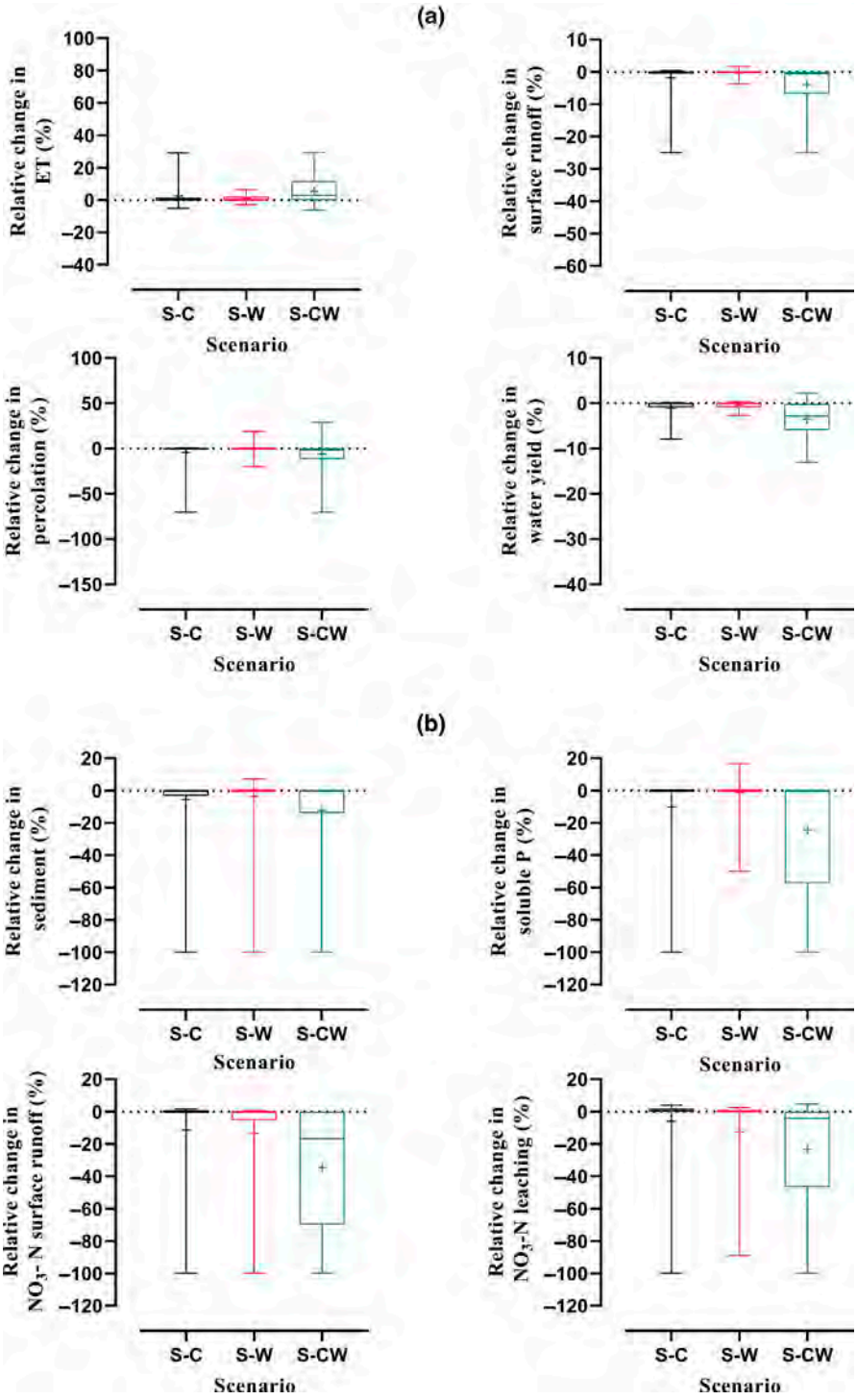

FIGURE 4 Box plots of average monthly relative changes (%) from 1997 to 2005 (December–May) in water balance components (a): evapotranspiration (ET), surface runoff, percolation, and water yield, and (b) total sediment load, soluble phosphorus (P) in surface runoff, nitrate (NO_3-N) in surface runoff, and NO_3-N leaching from the bottom of the soil profile at the watershed outlet under three different scenarios. The whiskers represent maximum and minimum, and "+" represents mean. S-C, stand-alone carinata; S-CW, rotating carinata and winter wheat; S-W, stand-alone winter wheat

show the simulated hydrology and water quality effects on the cotton and peanut HRUs during winter growing seasons under S-C, S-W, and S-CW scenarios. Simulated monthly average of ET, surface runoff, percolation, and water yield for cotton and peanut HRUs from 1997 to 2005 under baseline and S-C, S-W, and S-CW scenarios are presented in the Supporting Information (Figure S2).

Conversion of fallow lands to carinata, winter wheat, and combined carinata and winter wheat led to increased monthly ET and decreased runoff (water yield) from the cotton and peanut HRUs. The average annual (1997–2005) ET within the cotton and peanut HRUs was slightly increased from 671 mm for the baseline to 690.8 mm (2.8%), 682.9 mm (1.6%), and 674.6 mm (0.4%) for S-CW, S-C, and S-W scenarios, respectively (Table 4b). The highest increase in monthly average (December–May) ET relative to the baseline model was observed under S-CW when compared to S-C and S-W scenarios with the mean of 17.0 ± 3.0%, 7.0 ± 2.6%, and 3.0 ± 1.0%, respectively (Figure 5a). The ET reduction reached the lowest amount

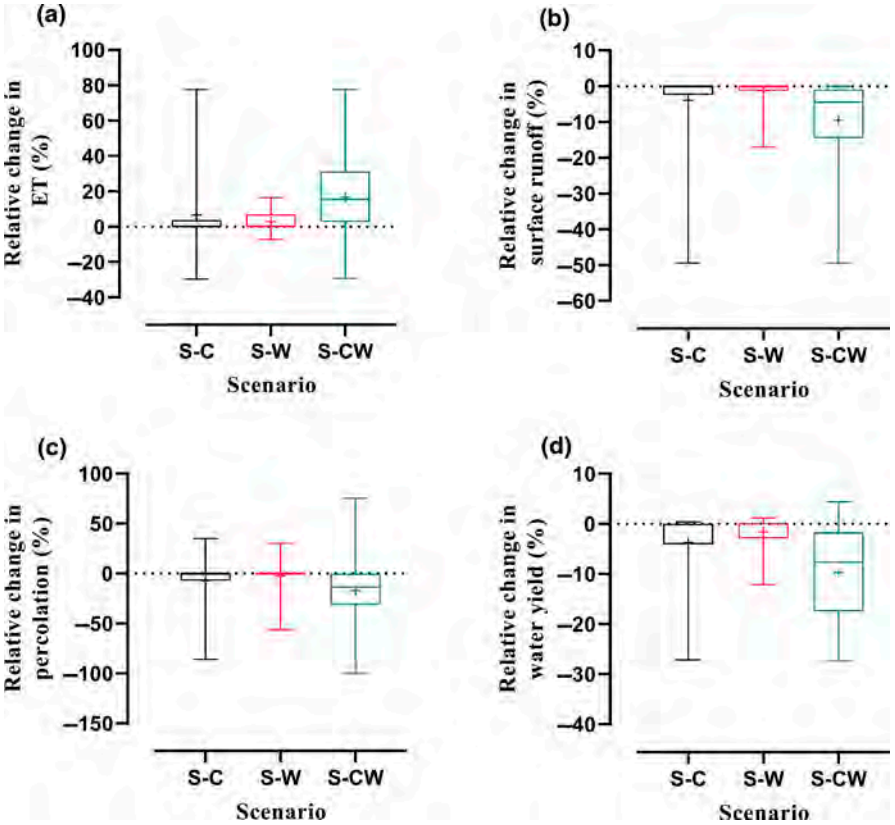

FIGURE 5 Box plots of relative changes (%) in average monthly (December–May) water balance components; evapotranspiration (ET; a), surface runoff (b), percolation (c), and water yield (d) from cotton and peanut HRUs (winter growing season) from 1997 to 2005 compared to the baseline model (winter fallow) under three different scenarios. The whiskers represent maximum and minimum, and "+" represents mean. S-C, stand-alone carinata, S-W, stand-alone winter wheat, and S-CW, rotating carinata and winter wheat

in May under all scenarios relative to the baseline model as a result of plant harvesting (Figure S2).

The changes in ET are reflected in surface runoff and water yield from HRUs, as more ET leads to less runoff and streamflow (Table 4b; Figure 5b). When compared to the baseline, the average annual (1997–2005) surface runoff and water yield from cotton and peanut HRUs reduced for all scenarios, with the highest reduction observed for the S-CW scenario (2.5% and 4.3%, respectively; Table 4b). Monthly average (December–May) surface runoff and water yield also decreased about 9.6 ± 1.6% and 9.7 ± 1.3% under S-CW, and 4.0 ± 1.4% and 3.7 ± 1.0% under S-C scenarios, respectively, followed by the S-W scenario (−1.3 ± 0.4% and −1.6 ± 0.5%; Figure 5b,d). A significant reduction in monthly water yield occurred in April and May as a result of surface runoff reduction (Figure S2). We did not observe any significant changes in ET for the following cotton and peanut summer crops for all three scenarios. Although surface runoff from following summer crop HRUs decreased by about 2.0 ± 0.5% under both S-CW and S-C scenarios compared to winter fallow. This is likely attributed to the plant residuals from the previous winter growing season (Figure S2). However, reduction in surface runoff from following summer crops HRUs under stand-alone winter wheat was negligible (less than 0.5%) compared to winter fallow (baseline)(Figure S2).

Under all three scenarios, average annual (1997–2005) percolation from cotton and peanut HRUs decreased within a range of 0.7%–5.4%, as compared to the winter fallow scenario (Table 4b). Following the same trend, the average monthly (December–May) water percolation past bottom of the soil profile also decreased for all three scenarios relative to the baseline, with the highest reduction of 17.0 ± 4.7% for S-CW scenario (Figure 5c). An increase in percolation was mainly observed in April and May with ET reduction, which can compensate the reduction in total water yield (Figure S2).

3.3.2 | Effects of carinata as a winter crop on TN, TP, and sediment loads

As expected, TN, TP, and sediment loadings from cotton and peanut HRUs from 1997 to 2005 also decreased when winter fallows were converted to carinata, winter wheat, and both carinata and winter wheat in rotation, with the impacts being relatively higher for S-CW scenario followed by S-C and S-W scenarios (Table 4b; Figures 5 and 7). Simulated average monthly loads for TN, TP, and sediment from cotton and peanut HRUs from 1997 to 2005 for the baseline condition and S-C, S-W, and S-CW are presented in the Supporting Information (Figure S3–S5).

The average annual (1997–2005) sediment, mineral P attached to sediment, soluble P, and NO_3-N loadings from the cotton and peanut HRUs under the baseline are estimated to be 4.7, 0.8, 0.3, and 5.5 tonne ha^{-1} $year^{-1}$ (Table 4b). There is a considerable decrease in average annual (1997–2005) total sediment (23%), mineral P transported by sediment

(50%), soluble P (67%), and NO_3-N in surface runoff (60%) loadings and leaching (44%) for S-CW scenario from cotton and peanut HRUs compared to the baseline (Table4b). Also, reduction in sediment loading was almost tripled under the S-C scenario (6%) compared to the S-W scenario (2%) (Table 4b). The sediment loading from the cotton and peanut HRUs from December to May (1997–2005), decreased with the reduction being almost doubled in S-C scenario with an average reduction of about 10.0 ± 2.9% compared to S-W scenario with an average reduction of 5.0 ± 1.5% (Figure 6a). Under these two scenarios, sediment loading was also slightly reduced from peanut HRUs following summer (1998, 2002, and 2005) with 5.0 ± 2.9% and 3.7 ± 2.2% reduction for S-C and S-W scenarios, respectively, compared to the baseline (winter fallow; Figure S3). Furthermore, when compared to the baseline, average monthly sediment loads from December to May (1997–2005) decreased from 0.013 to 0.009 tonne ha^{-1} day^{-1} (~−29.0 ± 3.2%) for S-CW (Figure 4a), and to 0.010 tones ha^{-1} day^{-1} (~−11.0 ± 2.5%) for the following cotton and peanut summer crops (Figure S3). Overall, the highest reduction in sediment loads from HRUs occurred in April and May due to the maximum aboveground and belowground plant development and runoff reduction.

The average monthly TP load into the stream from the cotton and peanut HRUs from December–May (1997–2005), reduced about 18.0 ± 3.5% and 17.0 ± 2.5% for S-C and S-W scenarios, respectively (Figure 6b). However, the average monthly TP load decreased by approximately 53.0 ± 3.5% under S-CW scenario (Figure 6b). The average monthly TP loading from the following cotton and peanut summer crops HRUs reduced 34.0 ± 2.8% under S-CW scenario, and 27.0 ± 2.9% under S-C, and 26.0 ± 2.4% under S-W scenarios (Figure S4a).

A close look at the TP load components showed that from 1997 to 2005, soluble P loss by surface runoff from the cotton and peanut HRUs reduced from 0.3 kg P ha^{-1} $year^{-1}$

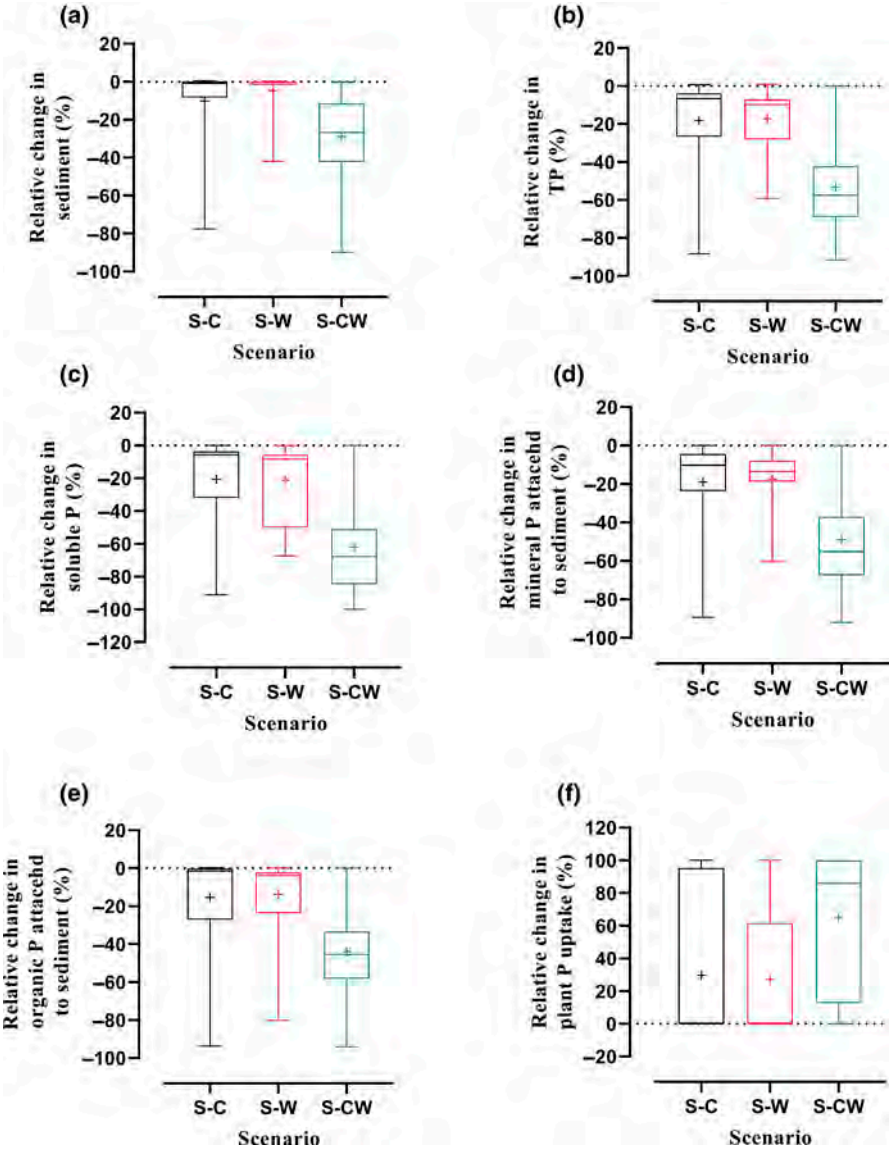

FIGURE 6 Box plots of relative changes (%) in average monthly (December–May) sediment (a), total phosphorus (TP)(b), soluble P (c), mineral P (d), and organic P (e) attached to sediment loadings, and plant P uptake (f) from cotton and peanut HRUs (winter growing season) from 1997 to 2005 compared to the baseline model (winter fallow) under three different scenarios. The whiskers represent maximum and minimum, and "+" represents mean. HRU, Hydrologic Response Unit; S-C, stand-alone carinata; S-CW, rotating carinata and winter wheat; S-W, stand-alone winter wheat

under baseline (winter fallow) to about 0.1 kg P ha^{-1} $year^{-1}$ (−67%) under S-CW scenario and 0.2 kg P ha^{-1} $year^{-1}$ (−33%) under S-C and S-W scenarios (Table 4b). The average monthly soluble P loading from December–May (1997–2005) to the stream also significantly decreased by about 21.0 ± 4.0% and 21.0 ± 3.2% under S-C and S-W scenarios, and 62.1 ± 4.2% under S-CW scenario relative to the baseline as a result of runoff reduction (Figure 6c). Under S-C and S-W scenarios, the estimated average monthly soluble P loading from the following peanut summer crop HRUs (1998, 2002, and 2005) also reduced by 39.0 ± 9.3% (S-W) and 36.0 ± 8.4% (S-C) compared to the baseline winter fallow (Figure S4b).

A similar trend was observed for mineral and organic P attached and transported by sediment from the cotton and peanut HRUs to the stream due to the reduction in sediment loads (Table 4b; Figure 6d,e). The average monthly mineral and organic P attached to sediment reduced by 19.0 ± 3.3% and 15.4 ± 3.6% for S-C, and 17.5 ± 2.3% and 13.0 ± 2.7% for S-W, respectively, from December to May (1997–2005) (Figure 6d,e). In contrast, the highest reduction of 49.0 ± 3.6% and 44 ± 3.4% in average monthly mineral and organic P loads was observed under S-CW scenario relative to the baseline from 1997 to 2005 (Figure 6d,e). Again, the highest reduction in TP, soluble P, organic P, and sediment P occurred in April and May due to runoff reduction (Figure S4). The soluble P, organic P loads and mineral P transported by sediment also decreased from the following cotton and peanut summer crops HRUs for S-CW scenario, approximately by 38.5 ± 4.0%, 12 ± 3.0%, and 39.4 ± 3.0%, respectively (Figure S4). Similarly, mineral P transported by sediment from the following peanut summer crop HRUs reduced from average

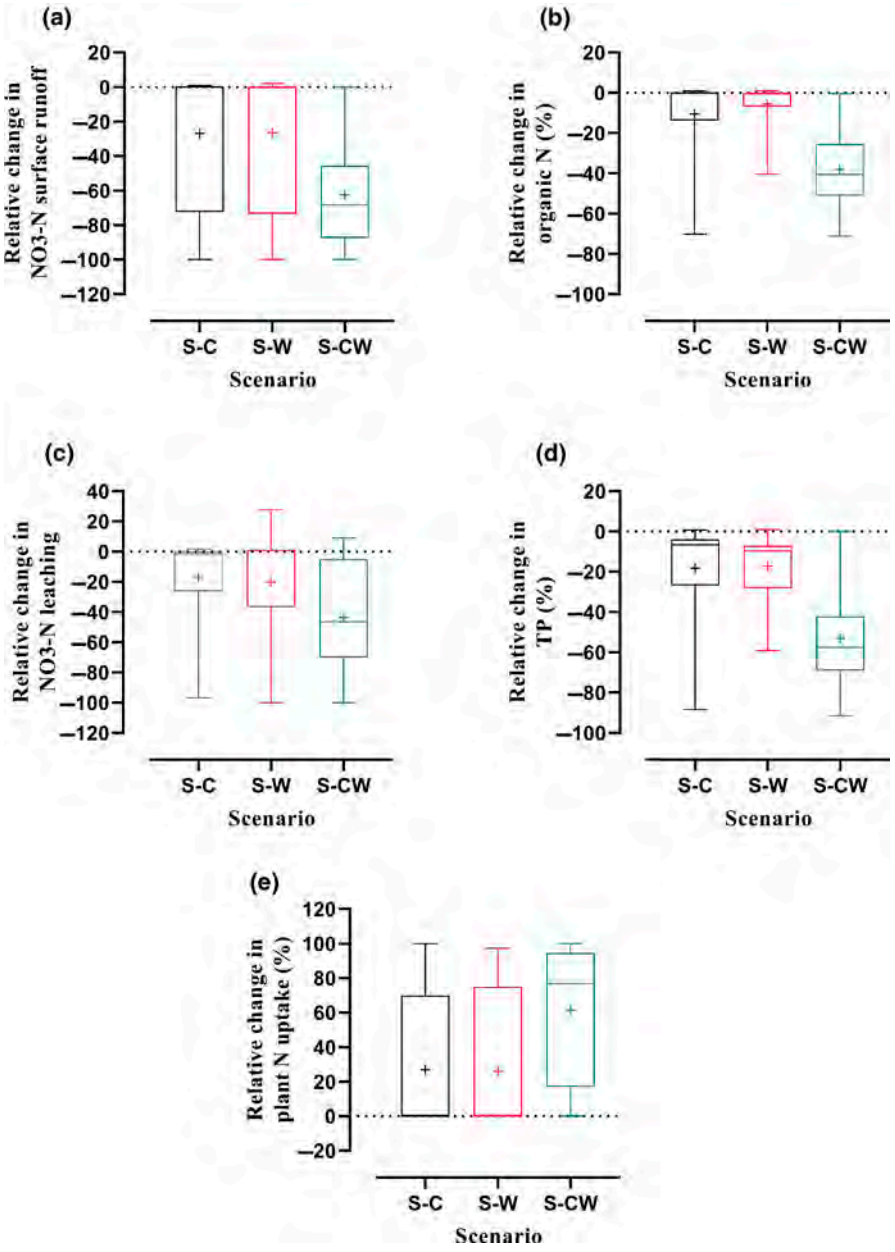

FIGURE 7 Box plots of relative changes (%) in average monthly (December–May) nitrate-nitrogen (NO_3-N) in surface runoff (a), organic N (b), NO_3-N in leaching (c), total N (TN)(d) and plant N uptake (e) from cotton and peanut HRUs (winter growing season) from 1997 to 2005 compared to the baseline model (winter fallow) under three different scenarios. The whiskers represent maximum and minimum, and "+" represents mean. S-C, stand-alone carinata; S-CW, rotating carinata and winter wheat; S-W, stand-alone winter wheat

0.0025 kg P ha^{-1} day^{-1} under the baseline (winter fallow) reduced to 0.0019 kg P ha^{-1} day^{-1} (−24.0 ± 2.4%) under S-C scenario and 0.0018 kg P ha^{-1} day^{-1} (−28.0 ± 1.7%) under S-W scenario (Figure S4c).

The average monthly NO_3-N and organic N loads in the surface runoff from the cotton and peanut HRUs from December–May (1997–2005) decreased by 27.0 ± 5.7% and 10.5 ± 2.9% under S-C scenario and 26.0 ± 5.6% and 5.5 ± 1.5% under S-W scenario, respectively, compared to the baseline (Figure 7a,b). Similarly, under the S-CW scenario, the average monthly NO_3-N and organic N loads in the surface runoff from the cotton and peanut HRUs from December to May (1997–2005) reduced by 63.0 ± 4.0%, 38.0 ± 2.7%, respectively, compared to the baseline (Figure 7a,b). Unlike sediment and TP loadings, under all three scenarios, there were no significant changes in average monthly NO_3-N and organic N loadings in the surface runoff from the following summer crops (Figure S5).

Reduction in percolation from the cotton and peanut HRUs from December to May (1997–2005) led to average monthly NO_3-N leaching reduced about 44.0 ± 5.0% for S-CW, followed by 19.1 ± 5.6% and 17.0 ± 4.2% for S-W and S-C scenarios, respectively compared to the baseline (Figure 7c). Overall, conversion of mainly fallow lands from the cotton and peanut HRUs to carinata (S-C), winter wheat (S-W), and combined carinata and winter wheat (S-CW) from December to May (1997–2005) led to the reduction in average TN load into the stream by 45.3 ± 3.5% (S-CW), 33.3 ± 5.3% (S-C), and 27.2 ± 5.0% (S-W) (Figure 7e). Reduction in TN load from the following summer crops was small and was about 2.0 ± 2.4% under S-CW and 2.0 ± 2.0% under S-C. However, TN load under stand-alone winter wheat scenario slightly increased (2.2 ± 2.0%) from the following summer crops compared to winter fallow (Figure S5a). Moreover, plant uptake of N and P from the cotton and peanut HRUs increased by about 61.4 ± 5.8%, 27.0 ± 5.7%, and 26.0 ± 5.7% for N, and 65.0 ± 6.1%, 30.0 ± 6.3%, and 27.0 ± 6.0% for P under S-CW, S-C, and S-W scenarios, respectively relative to the winter fallow (Figures 6f and 7d).

4 | DISCUSSION

4.1 | Evaluation of SWAT model performance

The simulated daily streamflow deemed "satisfactory" fit with daily observed streamflow during the calibration (1997–2001) period with a daily KGE of 0.75 and BPIAS of 5.1, and validation (2002–2005) period with the KGE of and PBIAS of −1.0 at the LREW outlet (Moriasi et al., 2015; Table 3; Figure 2). However, we observed some repeatable underpredications of streamflow during winter months during both calibration and validation periods (Figure 2). Underestimation of the peaks and overestimation of the hydrograph recession balances out the overall water-budget (Table 4). These SWAT simulation shortcomings for this watershed were first reported by Bosch et al. (2004). One potential reason for SWAT tendency to underpredict streamflow during wet winter months could be the adjustment for CN II (curve number moisture condition II) based on antecedent moisture conditions, which cannot accurately represent the seasonal variations in soil water storage in the studied watershed (Feyereisen et al., 2007).

In addition to the temporal accuracy of predicted streamflow at the watershed outlet, the spatial variability of simulated ET from 2000 to 2005 also showed acceptable variability with respect to the remotely sensed ET at the subbasin level. The calculated relative error for 184 out of 198 subbasins ranged from −20% to 20% with RMSE of 66 mm $year^{-1}$ (~ 9%; Figure S1).

The comparison of simulated average crop yields for the LREW with the crops yield reported by the University of Georgia Extension (UGA Extension, 2000) for Tifton County indicated that they both are in good coordinate with 4500 kg ha^{-1} for peanut and 2000 kg ha^{-1} for cotton for the study period.

Mean annual streamflow, sediment, TP, and NO_3-N loads are presented in Table 3. The model performance is considered "satisfactory" with daily KGE >0.45 and PBIAS ≤±20% for sediment load, with daily KGE >0.35 and PBIAS ≤±30% for TP load, and with daily KGE >0.35 and PBIAS ≤±30% for NO_3-N load (Moriasi et al., 2015). Therefore, the simulated daily sediment, TP, and NO_3-N loads of our SWAT model showed "satisfactory" to "good" agreement with observed values during calibration and validation at the outlet of the LREW (Table 3; Figure 3).

Parameter values should be considered after calibration to avoid unrealistic simulations. For instance, the fitted values for SOL_AWC in the SWAT model for crops and forest soil were ranging from 0.06 to 0.07 mm mm^{-1} that is comparable to the SOL_AWC weighted average of 0.057 mm mm^{-1} for the Tifton soil series reported by Hubbard (1985).

The simulated annual sediment load at the watershed outlet for the study period (1997–2005) was ranging from 1 to 4 metric tonne ha^{-1} $year^{-1}$ with an average of 2.6 tonne ha^{-1} (Table 4a). The measured total sediment load at the outlet of a small watershed with a drainage area of about 1.2 km^2 (Gibbs farm) located at the Tifton Upland physiographic region (only 12 km away from the LREW outlet) with similar land use, soils, and hydrogeology was ranging from 0.001 to 2.74 tonne ha^{-1} $year^{-1}$ from 1997–2003 with an average of 0.50 ± 0.80 tonne ha^{-1} (Lowrance et al., 2007). Bosch et al. (2020) reported 41 years of measured hydrologic and water quality data from the LREW

outlet. The average annual TP and NO_3-N loadings from 1990 to 1999 were about 0.25 ± 0.16 kg P ha^{-1} $year^{-1}$ and 1.05 ± 0.85 kg N ha^{-1} $year^{-1}$, respectively, and from 2000 to 2009, the average annual TP load was about 0.38 ± 0.43 kg P ha^{-1} $year^{-1}$, and average annual NO_3-N load 0.22 ± 0.21 for kg N ha^{-1} $year^{-1}$ (Bosch et al., 2020). The estimated average TP and NO_3-N loadings from the SWAT model at the outlet of LREW was 0.29 kg P ha^{-1} and 2.6 kg N ha^{-1}, respectively (Table 4a) that is comparable to measured loads by Bosch et al. (2020).

The simulated average annual sediment and NO_3-N loadings from our SWAT model were slightly overestimated, and it was at the upper end of the measured data (Table 4a). This is more likely attributed to disperse observed data from 1997 to 2003, resulting in higher PBIAS compared to streamflow (Table 3). However, the calibrated SWAT model predicted a denitrification rate of 0.04 kg ha^{-1} day^{-1} in the studied watershed, which is comparable to the average denitrification rate of 0.04 to 0.05 kg ha^{-1} day^{-1} for the study area (Lowrance et al., 1995; Vellidis, 1999).

4.2 | Potential benefits of converting winter fallow to carinata on hydrology

Average reductions in water yield were maximum for S-CW and S-C scenarios with approximately annual 2% and 1% reduction at the watershed outlet and 4% and 2% from the cotton and peanut HRUs, respectively (Table 4). This may point out that changes in aquatic environments are likely to be limited across the entire watershed and local scales, and it is proportional to the area converted to carinata and winter wheat. Therefore, a modest reduction in water yield was expected since only 12% and 36% of the total watershed area under S-C and S-CW scenarios, respectively, were converted to winter crops from 1997 to 2005. However, at the local level, the average water yield reductions for cotton and peanut HRUs in April and May were about 27%, which indicates the importance of local scale predicting and understanding of streamflow assessment in large-scale biofuel crop planting (Poff & Zimmerman, 2010). At both watershed and local scales, the dominant components in water yield reduction in the study watershed were water lost through ET. Physiological factors such as higher LAI of carinata resulted in higher water usage and higher ET than winter wheat during the winter growing season (Figure 5a).

On the other hand, the reduction in ET from the cotton and peanut HRUs in May for all scenarios compared to the baseline could be related to a reduction in transpiration due to plant harvest. Both carinata and winter wheat have almost similar HVSTIs of 0.35 and 0.40, respectively. Therefore, the plants residual after harvest affect the reduction in evaporation from soil surface compared to the winter fallow. The increase in ET is reflected in the surface runoff reduction. At the watershed outlet and local level, the reduction in simulated surface runoff was more apparent for S-C and S-CW scenarios compared to the S-W scenario (Table 4; Figure 5b). These may indicate the benefits of carinata over winter wheat in surface runoff reduction, which may result in less pollution loads into the stream.

We have to note that the simulated surface runoff in the SWAT model is based on the CN method (SCS, 1972) and Manning's roughness coefficients (Arcement & Schneider, 1989). The values for SCS runoff CN and Manning's roughness are well established for raw crops and traditional small grain winter crops, but empirical measurements are lacking for carinata. Therefore, we adopted these values for carinata similar to the spring canola from the same family (*B. napus)* in the LREW watershed.

4.3 | Potential benefits of converting winter fallow to carinata on sediment, TP, and TN loads

The average sediment loads from 1997 to 2005 decreased by more than double for stand-alone carinata scenario (S-C) compared to the S-W scenario at both the watershed outlet and the local level (Figures 4b and 6a). The higher reduction in sediment loading under S-C scenario than S-W scenario can be attributed to the relatively higher plant density of carinata than winter wheat. The bushy aboveground biomass of carinata reduced the power of rainfall to detach soil particles and reduce sediment load. The same reason is valid for S-CW scenario compared to the winter fallow (baseline condition). The minimal reduction in sediment loads under S-C and S-W scenarios from the winter fallow HRUs during consequent December-May (1999, 2002, and 2005) where neither carinata nor winter wheat was planted were more likely related to the accumulation of plant residual in soil from previous winter growing seasons. This reduction was higher for the S-C scenario than S-W, where carinata was planted. This can be confirmed by the reduction in simulated water yield from the winter fallow HRUs during the same periods (Figure S2).

The reduction in mineral P loadings in surface runoff (soluble P) at the watershed and local levels for all three scenarios is attributed to the reduction in runoff and increase in P uptake by plant with higher reduction observed at the HRU level (Figures 4b and 6c). For instance, at the local level plant P uptake increased from a monthly average of 0.007 kg ha^{-1} for the baseline to 0.065 kg P ha^{-1} for S-CW scenario, 0.054 kg P ha^{-1} for S-C scenario, and 0.032 kg P ha^{-1} for S-W scenario (Figure 6f). Moreover, organic P and mineral P loadings transported by sediment

into the stream decreased (Figure 6d,e) mainly due to the reduction in sediment loading from carinata and winter wheat HRUs (Figure 6a).

A slightly higher reduction in simulated TP loading from peanut and cotton HRUs after S-C scenario despite the application of mineral P fertilizer on carinata HRUs compared to S-W scenario (Figure 6b) is more likely due to a higher fraction of P in carinata yield than winter wheat yield (0.009 kg P kg^{-1} carinata yield vs. 0.002 kg P kg^{-1} winter wheat yield, respectively) (Kiniry et al., 1995; Seepaul et al., 2019). A close look into the benefits of converting winter fallow to carinata, winter wheat, and rotation of carinata and winter wheat (1997–2005) on the TP loading from the following summer crops indicated that TP loading from peanut and cotton HRUs reduced under all scenarios, due to reduction in mineral and organic P transported by sediment into the stream (Figure S4c,d). Overall, in the long term (1997–2005), converting winter fallow HRUs to stand-alone carinata (S-C) could reduce more TP loading into the stream than stand-alone winter wheat scenario (S-W), however the difference was minimal.

At the local level, the reduction in NO_3-N and organic N loadings in the surface runoff for all three scenarios compared to the baseline winter fallow was related to the reduction in the surface runoff, and thus decreased monthly average TN loading (Figure 7a, b, and d). At both watershed scale and local level, the reduction in NO_3-N load under S-C and S-W scenarios was similar when N fertilizer requirement of 90 kg N ha^{-1} was applied.

With the presence of carinata and winter wheat, NO_3-N leaching from the bottom of soil profile decreased mainly as a result of the increase in plant N uptake (Figure 7e). However, under S-W scenario, an increase in NO_3-N leaching (Figure 4c) could be attributed to a higher fraction of N in winter wheat biomass at plant maturity than N fraction in carinata biomass at maturity (0.015 kg N kg^{-1} winter wheat vs. 0.010 kg N kg^{-1} carinata, respectively) (Kiniry et al., 1995; Seepaul et al., 2019) which consequently might leave more N in the soil and make it more susceptible to N mineralization and leaching.

Compared to the benefits of carinata on NO_3-N loading at the local level, the simulated NO_3-N loading at the watershed scale was small mainly due to the importance of riparian forest buffers in removing N from the study watershed before reaching the outlet (Figures 4b and 7a).

It is important to note that the extent of total area converted to carinata, winter wheat, or both within the watershed is also critical in assessing the hydrologic and water quality benefits of carinata. We observed higher reductions in sediment, TP, and TN loads when 36% of the total watershed or 100% of cotton and peanut HRUs were converted to carinata and winter wheat rotation. In contrast, when only 12% of the total watershed area was converted to carinata or winter wheat (S-C and S-W scenarios, respectively), the reduction was modest.

In summary, we assessed the hydrologic and water quality benefits associated with land use change from winter fallow to carinata in the coastal plain of Georgia using the SWAT model. Our results indicated that ET could increase, and as a result, surface runoff and water yield decreased under S-C scenario, followed by S-W scenario relative to the baseline. A similar reduction trend was observed for sediment loads and mineral P and organic P transported by sediments into the stream when stand-alone carinata compared to stand-alone winter wheat. In addition, converting winter fallow to stand-alone carinata resulted in a higher reduction of organic nitrogen loading into the stream than the stand-alone winter wheat scenario. Also, NO_3-N loading reduction through surface runoff under both S-C and S-W scenarios relative to the baseline was almost the same.

We conclude that our results are consistent with a mechanistic understanding of the benefits of carinata on water quality and indicate that carinata can be planted as a promising winter biofuel crop in south-central Georgia while providing winter crop benefits in rotations. We observed more significant benefits in surface runoff reduction, and consequently, reduction in sediment, TP, and TP loadings into the stream when carinata was planted instead of winter wheat. Moreover, we observed the highest benefits of converting fallow land to carinata on TN, TP, and sediment loads when carinata was in rotation with winter wheat.

Minimal nutrient load reductions in the study watershed can be explained by the extent to which total area converted to carinata across the watershed, coupled with the fact that LREW is a heavily buffered system.

From a broader nutrient management perspective, we expect that substantial reduction in sediment, TP, and TN loads would be observed when planting carinata as a winter crop combined with other nutrient management implementations such as developing best management practice at agricultural fields and fertilizer management. This might be critical in regions where excess phosphorus and nitrogen concentrations in streams may lead to excessive algal growth and eutrophication of freshwater ecosystems.

Here, we included relevant biophysical parameters during the streamflow calibration process using the aggregated (or lumped) approach (Chen et al., 2017; Cibin et al., 2016; Demissie et al., 2017; Holder et al., 2019). Recent research in watershed modeling has shown improvements in hydrology and water quality predictions with the assimilation of remotely sensed biophysical data (e.g., LAI; Ma et al., 2019; Rajib et al., 2020). Future research is needed to incorporate remotely sensed biophysical parameters in modeling the effect of bioenergy crops on hydrology and water quality with respect to crop yields in various geophysical regions.

We need to point out the potential uncertainties associated with the carinata modeling hydrology components

(such as surface runoff), nutrients, and sediment loads, as no measurements were available for the model evaluation at this time. Field experiments should be performed to assess water quantity and quality impacts of carinata scenarios directly. Also, the associated cost (seed cost, fertilization, fuel, etc.) to planting carinata and winter wheat as a winter crop needs to be weighed against water quality benefits. In addition, this finding may be transferable to watersheds with similar specific characteristics and management practices.

Further research is needed to better understand the effects of carinata on hydrology, nutrient, and sediment loads in nested watersheds within the southeast US and various management practices.

ACKNOWLEDGMENTS

We would like to thank the United States Department of Agriculture National Institute of Food and Agriculture (USDA-NIFA) for their support throughout this project. Also, we would like to acknowledge Dr. Dewey Lee, University of Georgia Extension Agronomist, and Dr. Ramdeo Seepaul at the University of Florida, North Florida Research and Education Center, Quincy, FL for providing essential information throughout this project. This work was supported by USDA-NIFA Coordinated Agriculture project grant program (grant no. SRD0007 and USDA-NIFA project no. 2016-11231) Southeast Partnership for Advanced Renewables from Carinata.

DATA AVAILABILITY STATEMENT

The data that support the findings of this study are available from the corresponding author upon reasonable request.

ORCID

Nahal Hoghooghi https://orcid.org/0000-0002-1629-8863

REFERENCES

Abbaspour, K. (2013). *SWAT-CUP 2012: SWAT calibration and uncertainty programs-A user manual*. Eawag Swiss Federal Institute of Aquatic Science and Technology.

Abbaspour, K. C., Yang, J., Maximov, I., Siber, R., Bogner, K., Mieleitner, J., Zobrist, J., & Srinivasan, R. (2007). Modelling hydrology and water quality in the pre-alpine/alpine Thur watershed using SWAT. *Journal of Hydrology*, *333*, 413–430. https://doi.org/10.1016/j.jhydrol.2006.09.014

Agrisoma. (2017–18). *Carinata managment handbook*. Retrieved from https://agrisoma.com/wp-content/uploads/2018/10/2017_18_SE_Handbook.pdf

Arcement, G. J., & Schneider, V. R. (1989). *Guide for selecting Manning's roughness coefficients for natural channels and flood plains*. US Government Printing Office. Retrieved from https://dpw.lacounty.gov/lacfcd/wdr/files/WG/041615/Guide%20for%20Selecting%20n-Value.pdf

Arnold, J., Allen, P., Muttiah, R., & Bernhardt, G. (1995). Automated base flow separation and recession analysis techniques. *Groundwater*, *33*, 1010–1018. https://doi.org/10.1111/j.1745-6584.1995.tb00046.x

Arnold, J., Kiniry, J., Srinivasan, R., Williams, J., Haney, E., & Neitsch, S. (2013). *SWAT 2012 input/output documentation*. Texas Water Resources Institute, 654 pp.

Arnold, J., Moriasi, D., Gassman, P., Abbaspour, K., White, M., Srinivasan, R., Santhi, C., Harmel, R., Van Griensven, A., & Van Liew, M. (2012). SWAT: Model use, calibration, and validation. *Transactions of the ASABE*, *55*, 1491–1508. https://doi.org/10.13031/2013.42256

Baggs, E., Watson, C., & Rees, R. (2000). The fate of nitrogen from incorporated cover crop and green manure residues. *Nutrient Cycling in Agroecosystems*, *56*, 153–163. https://doi.org/10.1023/a:1009825606341

Bosch, D., Pisani, O., Coffin, A., & Strickland, T. (2020). Water quality and land cover in the Coastal Plain Little River watershed, Georgia, United States. *Journal of Soil and Water Conservation*, *75*, 263–277. https://doi.org/10.2489/jswc.75.3.263.

Bosch, D. D., Sheridan, J., Batten, H., & Arnold, J. (2004). Evaluation of the SWAT model on a coastal plain agricultural watershed. *Transactions of the ASAE*, *47*, 1493–1506. https://doi.org/10.13031/2013.17629

Bosch, D., Sheridan, J., & Davis, F. (1999). Rainfall characteristics and spatial correlation for the Georgia Coastal Plain. *Transactions of the ASAE*, *42*, 1637–1644. https://doi.org/10.13031/2013.13330

Bosch, D., Sheridan, J., Lowrance, R., Hubbard, R., Strickland, T., Feyereisen, G., & Sullivan, D. (2007). Little river experimental watershed database. *Water Resources Research*, *43*. https://doi.org/10.1029/2006WR005844

Chen, Y., Ale, S., Rajan, N., & Munster, C. (2017). Assessing the hydrologic and water quality impacts of biofuel-induced changes in land use and management. *GCB Bioenergy*, *9*, 1461–1475. https://doi.org/10.1111/gcbb.12434

Cho, J., Vellidis, G., Bosch, D. D., Lowrance, R., & Strickland, T. (2010). Water quality effects of simulated conservation practice scenarios in the Little River Experimental watershed. *Journal of Soil and Water Conservation*, *65*(6), 463–473. https://doi.org/10.2489/jswc.65.6.463

Christ, B., Bartels, W.-L., Broughton, D., Seepaul, R., & Geller, D. (2020). In pursuit of a homegrown biofuel: Navigating systems of partnership, stakeholder knowledge, and adoption of *Brassica carinata* in the Southeast United States. *Energy Research & Social Science*, *70*, 101665. https://doi.org/10.1016/j.erss.2020.101665

Cibin, R., Trybula, E., Chaubey, I., Brouder, S. M., & Volenec, J. J. (2016). Watershed-scale impacts of bioenergy crops on hydrology and water quality using improved SWAT model. *GCB Bioenergy*, *8*, 837–848. https://doi.org/10.1111/gcbb.12307

Demissie, Y., Yan, E., & Wu, M. (2017). Hydrologic and water quality impacts of biofuel feedstock production in the Ohio River Basin. *GCB Bioenergy*, *9*, 1736–1750. https://doi.org/10.1111/gcbb.12466.

Engel, B., Chaubey, I., Thomas, M., Saraswat, D., Murphy, P., & Bhaduri, B. (2010). Biofuels and water quality: Challenges and opportunities for simulation modeling. *Biofuels*, *1*, 463–477. https://doi.org/10.4155/bfs.10.17

Feyereisen, G., Strickland, T., Bosch, D., & Sullivan, D. (2007). Evaluation of SWAT manual calibration and input parameter sensitivity in the Little River watershed. *Transactions of the ASABE*, *50*, 843–855. https://doi.org/10.13031/2013.23149

Gerbrandt, K., Chu, P. L., Simmonds, A., Mullins, K. A., MacLean, H. L., Griffin, W. M., & Saville, B. A. (2016). Life cycle assessment of lignocellulosic ethanol: A review of key factors and methods affecting calculated GHG emissions and energy use. *Current Opinion in Biotechnology*, *38*, 63–70. https://doi.org/10.1016/j.copbio.2015.12.021

Greene, M. I. (2017). *Conversion of triacylglycerides-containing oils*. Chevron Lummus Global, LLC; Applied Research Associate Inc. US 9,162.938 B2 p. 10. Retrieved from https://patentimages.storage.googleapis.com/a0/c9/c2/201bcb8e55bc05/US9162938.pdf https://patents.google.com/patent/US9162938

Guo, T., Cibin, R., Chaubey, I., Gitau, M., Arnold, J. G., Srinivasan, R., Kiniry, J. R., & Engel, B. A. (2018). Evaluation of bioenergy crop growth and the impacts of bioenergy crops on streamflow, tile drain flow and nutrient losses in an extensively tile-drained watershed using SWAT. *Science of the Total Environment*, *613–614*, 724–735. https://doi.org/10.1016/j.scitotenv.2017.09.148

Gupta, H. V., Kling, H., Yilmaz, K. K., & Martinez, G. F. (2009). Decomposition of the mean squared error and NSE performance criteria: Implications for improving hydrological modelling. *Journal of Hydrology*, *377*, 80–91. https://doi.org/10.1016/j.jhydrol.2009.08.003

Haramoto, E. R., & Gallandt, E. R. (2004). Brassica cover cropping for weed management: A review. *Renewable Agriculture and Food Systems*, *19*, 187–198. https://doi.org/10.1079/RAFS200490

Hargreaves, G. L., Hargreaves, G. H., & Riley, J. P. (1985). Agricultural benefits for Senegal River basin. *Journal of Irrigation and Drainage Engineering*, *111*, 113–124. https://doi.org/10.1061/(ASCE)0733-9437

Herman, M. R., Nejadhashemi, A. P., Abouali, M., Hernandez-Suarez, J. S., Daneshvar, F., Zhang, Z., Anderson, M. C., Sadeghi, A. M., Hain, C. R., & Sharifi, A. (2018). Evaluating the role of evapotranspiration remote sensing data in improving hydrological modeling predictability. *Journal of Hydrology*, *556*, 39–49. https://doi.org/10.1016/j.jhydrol.2017.11.009

Hoekman, S. K., Broch, A., & Liu, X. V. (2018). Environmental implications of higher ethanol production and use in the US: A literature review. Part I – Impacts on water, soil, and air quality. *Renewable and Sustainable Energy Reviews*, *81*, 3140–3158. https://doi.org/10.1016/j.rser.2017.05.050

Holder, A. J., Rowe, R., McNamara, N. P., Donnison, I. S., & McCalmont, J. P. (2019). Soil & Water Assessment Tool (SWAT) simulated hydrological impacts of land use change from temperate grassland to energy crops: A case study in western UK. *Global Change Biology: Bioenergy*, *11*, 1298–1317. https://doi.org/10.1111/gcbb.12628

Hubbard, R. (1985). *Characteristics of selected upland soils of the Georgia Coastal Plain*. USDA-ARS, ARS-37.

Isse, A., MacKenzie, A. F., Stewart, K., Cloutier, D. C., & Smith, D. L. (1999). Cover crops and nutrient retention for subsequent sweet corn production. *Agronomy Journal*, *91*, 934–939. https://doi.org/10.2134/agronj1999.916934x

Kiniry, J. R., Williams, J. R., Major, D., Izaurralde, R., Gassman, P. W., Morrison, M., Bergentine, R., & Zentner, R. (1995). EPIC model parameters for cereal, oilseed, and forage crops in the northern Great Plains region. *Canadian Journal of Plant Science*, *75*, 679–688. https://doi.org/10.4141/cjps95-114

Liew, M. W. V., Arnold, J. G., & Bosch, D. D. (2005). Problems and potential of autocalibrating a hydrologic model. *American Society of Agricultural Engineers*, *48*, 1025–1040. https://doi.org/10.13031/2013.18514

Lowrance, R., Sheridan, J., Williams, R., Bosch, D., Sullivan, D., Blanchett, D., Hargett, L., & Clegg, C. (2007). Water quality and hydrology in farm-scale coastal plain watersheds: Effects of agriculture, impoundments, and riparian zones. *Journal of Soil and Water Conservation*, *62*, 65–76.

Lowrance, R., Vellidis, G., & Hubbard, R. K. (1995). Denitrification in a restored riparian forest wetland. *Journal of Environmental Quality*, *24*, 808–815. https://doi.org/10.2134/jeq1995.00472425002400050003x

Ma, T., Duan, Z., Li, R., & Song, X. (2019). Enhancing SWAT with remotely sensed LAI for improved modelling of ecohydrological process in subtropics. *Journal of Hydrology*, *570*, 802–815.

Miguez, F. E., Maughan, M., Bollero, G. A., & Long, S. P. (2012). Modeling spatial and dynamic variation in growth, yield, and yield stability of the bioenergy crops *Miscanthus* × *giganteus* and *Panicum virgatum* across the conterminous United States. *GCB Bioenergy*, *4*, 509–520. https://doi.org/10.1111/j.1757-1707.2011.01150.x

Moriasi, D. N., Arnold, J. G., Van Liew, M. W., Bingner, R. L., Harmel, R. D., & Veith, T. L. (2007). Model evaluation guidelines for systematic quantification of accuracy in watershed simulations. *Transactions of the ASABE*, *50*, 885–900. https://doi.org/10.13031/2013.23153

Moriasi, D. N., Gitau, M. W., Pai, N., & Daggupati, P. (2015). Hydrologic and water quality models: Performance measures and evaluation criteria. *Transactions of the ASABE*, *58*, 1763–1785. https://doi.org/10.13031/trans.58.10715

Moriasi, D., Wilson, B., Douglas-Mankin, K., Arnold, J., & Gowda, P. (2012). Hydrologic and water quality models: Use, calibration, and validation. *Transactions of the ASABE*, *55*, 1241–1247. https://doi.org/10.13031/2013.42265

Nash, J. E., & Sutcliffe, J. V. (1970). River flow forecasting through conceptual models part I – A discussion of principles. *Journal of Hydrology*, *10*, 282–290. https://doi.org/10.1016/0022-1694(70)90255-6

NCEP. (2014). *Global weather data of SWAT*. National Centers for Environmental Prediction (NCEP); Climate Forcast System Reanalysis (CFSR). https://globalweather.tamu.edu/#pubs

Ng, T. L., Eheart, J. W., Cai, X., & Miguez, F. (2010). Modeling *Miscanthus* in the soil and water assessment tool (SWAT) to simulate its water quality effects as a bioenergy crop. *Environmental Science & Technology*, *44*, 7138–7144. https://doi.org/10.1021/es9039677

Poff, N. L., & Zimmerman, J. K. (2010). Ecological responses to altered flow regimes: A literature review to inform the science and management of environmental flows. *Freshwater Biology*, *55*, 194–205. https://doi.org/10.1111/j.1365-2427.2009.02272.x

Rajib, A., Evenson, G. R., Golden, H. E., & Lane, C. R. (2018). Hydrologic model predictability improves with spatially explicit calibration using remotely sensed evapotranspiration and biophysical parameters. *Journal of Hydrology*, *567*, 668–683. https://doi.org/10.1016/j.jhydrol.2018.10.024

Rajib, A., Kim, I. L., Golden, H. E., Lane, C. R., Kumar, S. V., Yu, Z., & Jeyalakshmi, S. (2020). Watershed modeling with remotely sensed big data: MODIS leaf area index improves hydrology and water quality predictions. *Remote Sensing*, *12*, 2148. https://doi.org/10.3390/rs12132148

Running, S., Mu, Q., Zhao, M., & Moreno, A. (2019). *MOD16A3GF MODIS/Terra Net Evapotranspiration Gap-Filled Yearly L4*

Global 500 m SIN Grid V006. NASA EOSDIS Land Processes DAAC. https://doi.org/10.5067/MODIS/MOD16A3GF.006 s

Schulmeister, T. M., Ruiz-Moreno, M., Silva, G. M., Garcia-Ascolani, M., Ciriaco, F. M., Henry, D. D., Lamb, G. C., Dubeux Jr., J. C., & Dilorenzo, N. (2019). Evaluation of *Brassica carinata* meal as a protein supplement for growing beef heifers. *Journal of Animal Science*, *97*, 4334–4340. https://doi.org/10.1093/jas/skz280

SCS. (1972). *Soil conservation services, national engineering handbook, section 4: Hydrology. National engineering handbook*, Washington, DC: US Department of Agriculture, SCS.: . US Department of Agriculture, SCS. https://directives.sc.egov.usda.gov/OpenNonWebContent.aspx?content=18393.wba

Seepaul, R. (2018–19). Carinata biophysical parameters. To: nahalh@uga.edu. Personal communication.

Seepaul, R., Bliss, C., Wright, D., Marois, J., Leon, R., Dufault, N., George, S., & Olson, S. (2016). *Carinata, the jet fuel cover crop: 2016 production manual for the Southeasten United States*. SSAGR-384. University of Florida/Institute of Food and Agricultural Sciences Extension Service. https://sparc-cap.org/wp-content/uploads/2018/04/Production-manual-2016.pdf

Seepaul, R., Marois, J., Small, I. M., George, S., & Wright, D. L. (2019). Carinata dry matter accumulation and nutrient uptake responses to nitrogen fertilization. *Agronomy Journal*, *111*, 2038–2046. https://doi.org/10.2134/agronj2018.10.0678

Seepaul, R., Mulvaney, M. J., Small, I. M., George, S., & Wright, D. L. (2020). Carinata growth, yield and chemical composition responses to nitrogen fertilizer management. *Agronomy Journal*, *112*, 5249–5263. https://doi.org/10.1002/agj2.20416

Shah, S., Hookway, S., Pullen, H., Clarke, T., Wilkinson, S., Reeve, V., & Fletcher, J. (2017). The role of cover crops in reducing nitrate leaching and increasing soil organic matter. *Aspects of Applied Biology*, *134*, 243–251.

Sharpley, A., Smith, S., & Hargrove, W. (1991). *Effects of cover crops on surface water quality*, The Proceedings of an International Conference, Cover crops for clean water, Jackson, Tennessee. April 9–11, (41–49). Soil and Water Conserv. Soc. http://citeseerx.ist.psu.edu/viewdoc/download?doi=10.1.1.596.3210&rep=rep1&type=pdf

Shrestha, D., Staab, B., & Duffield, J. (2019). Biofuel impact on food prices index and land use change. *Biomass and Bioenergy*, *124*, 43–53. https://doi.org/10.1016/j.biombioe.2019.03.003

Simpson, T. W., Sharpley, A. N., Howarth, R. W., Paerl, H. W., & Mankin, K. R. (2008). The new gold rush: Fueling ethanol production while protecting water quality. *Journal of Environmental Quality*, *37*, 318–324. https://doi.org/10.2134/jeq2007.0599

Trybula, E. M., Cibin, R., Burks, J. L., Chaubey, I., Brouder, S. M., & Volenec, J. J. (2015). Perennial rhizomatous grasses as bioenergy feedstock in SWAT: Parameter development and model improvement. *GCB Bioenergy*, *7*, 1185–1202. https://doi.org/10.1111/gcbb.12210

UGA Extension. (1999). *University of Georgia Cooperative Extension small grains performance test*. Retrieved from https://extension.uga.edu/publications/detail.html?number=RR666#Wheat

UGA Extension. (2000). *Field crops, forage, and turfgrass production*. Retrieved from https://extension.uga.edu/publications/browse.html?keywordTypeID=65&keywordType=Field+Crops%2C+Forage+and+Turfgrass+Production

UGA Extension. (2005). *University of Georgia Cooperative Extension crops performance test 2018*. Retrieved from https://www.caes.uga.edu/extension-outreach.html

USDA. (2010). *A USDA regional roadmap to meeting the biofuels goals of the renewable fuels standard by 2022*. US Department of Agriculture. Retrieved from https://www.USDA.gov/sites/default/files/documents/USDA_Biofuels_Report_6232010.pdf

Vellidis, G. (1999). *Water quality function of riparian ecosystems in Georgia*. Georgia Water Resources Conference, Athens, GA. March 30–31. Georgia Institute of Technology. 207–210. https://smartech.gatech.edu/bitstream/handle/1853/47503/VellidisG-99.pdf?sequence=1&isAllowed=y

Yasumoto, S., Suzuki, K., Matsuzaki, M., Hiradate, S., Oose, K., Hirokane, H., & Okada, K. (2011). Effects of plant residue, root exudate and juvenile plants of rapeseed (*Brassica napus* L.) on the germination, growth, yield, and quality of subsequent crops in successive and rotational cropping systems. *Plant Production Science*, *14*, 339–348. https://doi.org/10.1626/pps.14.339

SUPPORTING INFORMATION

Additional supporting information may be found online in the Supporting Information section.

How to cite this article: Hoghooghi N, Bosch DD, Bledsoe BP. Assessing hydrologic and water quality effects of land use conversion to *Brassica carinata* as a winter biofuel crop in the southeastern coastal plain of Georgia, USA using the SWAT model. *GCB Bioenergy*. 2020;00:1–20. https://doi.org/10.1111/gcbb.12792